Journal of Geoscience and Environment Protection, 2025, 13(8), 321-352
https://www.scirp.org/journal/gep
ISSN Online: 2327-4344
ISSN Print: 2327-4336

Infiltrability Variations on Surface Features of Sahelian Soils around Niamey (Southwestern Niger)

Harouna Amadou Harouna[1*], Amadou Abdourhamane Toure[1], Moussa Boubacar Moussa[1], Manuela Grippa[2], Salifou Noma Adamou[1], Bouba Hassane[1], Issoufou Ide[1]

[1]Department of Geology, Faculty of Science and Technology, Abdou Moumouni University, Niamey, Niger
[2]Geosciences Environnement Toulouse (UPS, CNRS, IRD), Toulouse, France
Email: *harounaamadouh@gmail.com

How to cite this paper: Harouna, H. A., Toure, A. A., Moussa, M. B., Grippa, M., Adamou, S. N., Hassane, B., & Ide, I. (2025). Infiltrability Variations on Surface Features of Sahelian Soils around Niamey (Southwestern Niger). *Journal of Geoscience and Environment Protection, 13,* 321-352.
https://doi.org/10.4236/gep.2025.138017

Received: July 12, 2025
Accepted: August 26, 2025
Published: August 29, 2025

Copyright © 2025 by author(s) and Scientific Research Publishing Inc.
This work is licensed under the Creative Commons Attribution International License (CC BY 4.0).
http://creativecommons.org/licenses/by/4.0/
Open Access

Abstract

The Sahel is confronting hydrological modifications resulting from changes in surface features and soil degradation. Efficient soil management requires characterization of the hydrodynamics of surface features, which are highly diversified. The aim of this study was to assess the hydraulic conductivity of encrusted surfaces, undegraded surfaces, sown surfaces, walking paths of irrigated perimeters, and the bottoms of koris. These surface features are widespread in the central Sahel and in the study site, which is the complex of lakes on the eastern-northeastern periphery of the city of Niamey. The approach was based on measuring hydraulic conductivity using the BEST method and determining the physical parameters of the soils in the various surface features. In all the surface features analyzed, the soils were composed of at least 95% sand, with a very low fine clay-loam fraction, often well below 5%. Higher values of the very fine to fine sands fraction and of the clay-loam fraction tend to reduce hydraulic conductivity. On the contrary, the latter increases with increasing soil density, despite its low variability (1.31 - 1.49 $g{\cdot}m^{-3}$). Hydraulic conductivity is highest in the koris (4.6×10^{-2} $mm{\cdot}s^{-1} \pm 4.6 \times 10^{-2}$) and lowest ($9.7 \times 10^{-4}$ $mm{\cdot}s^{-1} \pm 5.1 \times 10^{-4}$) on the crusted surfaces above the plateaus. With rainfall intensities varying between 1.39×10^{-5} and 0.25 $mm{\cdot}s^{-1}$ in the area, almost 90% of the rainfall that falls on the plateaus runs off, causing severe erosion on the glacis. To combat this erosion, bench-type devices are built to store water on the plateau. Given the very low infiltrability of plateau soils, it is advisable to use soil management that slows runoff instead of that which stores water, which makes it prone to evaporation.

Keywords

Surface Features, Hydraulic Conductivity, Soils, Niamey, Sahel

1. Introduction

The Sahel is highly sensitive to global change (L'Hôte et al., 2002; Hiernaux & Le Houérou, 2006; Amogu, 2009; Atta et al., 2010; Panthou et al., 2014; Taylor et al., 2017; Brüning & Piquet, 2018; Vischel et al., 2019). Annual rainfall amounts were abundant between 1930 and 1960. By the end of the 1980s, the isohyets had retreated by 200 km to the south and, in some areas, had fallen by as much as 200 mm, a decrease of 25 to 40% compared with the 1930-1960 period (Lebel & Ali, 2009; Nicholson, 2011; Potts & Graves, 2013; Kabore et al., 2017). Rainfall deficits and droughts have led to the degradation of Sahelian environments, with the deaths of many people and animals, the loss of millions of trees (Ambouta, 2007; Ballouche & Taïbi, 2013; Moussa Issaka, 2014; Ozer & Perrin 2014; Millogo et al., 2017) and changes in the surface runoff system (Sighomnou et al., 2013; Gal et al., 2017; Descroix et al., 2018). A gradual return of rainfall has been observed since the 1990s. Moreover, over the last 4 decades, maximum annual rainfall intensities have increased by an average of 2-6% per decade (Descroix et al., 2015; Malam Abdou, 2016; Panthou et al., 2018).

The Sahelian environment has also been impacted by strong anthropogenic pressure. Indeed, the Sahel is the region of the world with the highest annual population growth (3.9%) (Garenne & Ferdi, 2016; Oumani, 2023). Niger, for example, has the world's highest population growth rate (4%) and fertility rate (6.2 children per woman) (INS-Niger, 2018; Oumani, 2023). These high rates have led to a doubling of Niger's population every 20 years. High population growth has led to an extension of cultivated areas and an increase in deforestation in several areas (Guengant & Banoin, 2003; Moussa Issaka, 2014; Mamadou et al., 2015). The extension of cultivated areas has been to the detriment of natural wooded areas and fallow land (Abdourhamane Touré, 2011; Robert et al., 2017; Maigari et al., 2018). In southwest Niger, for example, cultivated areas increased by 80% in Fakara between 1950 and 2000 (Leblanc et al., 2007), 24% between 1994 and 2006 (Hiernaux et al., 2009); by 48.7% in Saga Gorou between 1950 and 1975 (Abdourhamane Touré et al., 2011), and by almost 50% in the Ouallam kori zone between 1972 and 2019 (Noma Adamou et al., 2024b). Soils in this area are sandy and particularly sensitive to erosion (Rajot et al., 2009; Abdourhamane Touré et al., 2018; Noma Adamou et al., 2022). In south-western Niger, for example, wind erosion causes land losses of 20 $t \cdot ha^{-1} \cdot yr^{-1}$ on cultivated areas (Abdourhamane Touré, 2011), while water erosion causes average losses ranging from 1.54 $t \cdot ha^{-1} \cdot yr^{-1}$ (Noma Adamou et al., 2022) to 1.92 $t \cdot ha^{-1} \cdot yr^{-1}$ (Descroix et al., 2012). Overall, more than 100,000 ha of arable land are lost every year in Niger (Folega et al., 2019; Mahamadou et al., 2023; Mahamadou Moudi et al., 2024). These soil losses deteriorate the soil properties (Kinnell, 2012; Rienzi et al., 2013; Li & Fang, 2016; Liu et al., 2019) and cause a decrease in soil productive potential, loss of biodiversity and soil surface crusting (Mamadou, 2012; Abdourhamane Touré et al., 2010; Abdourhamane Touré et al., 2017). Soil crusting is the most severe form of degradation in Sahelian soils (Malam Issa et al., 1999; Habou et al., 2016). It modifies the hydrodynamic

properties of the soil surface, in particular infiltration and runoff (Ambouta et al., 1996; Malam Issa et al., 2009; Malam Issa et al., 2011; Yeom, 2017). Surface features can therefore evolve in space and time under the influence of soil and climatic factors, in particular water and wind erosion (Valentin & Bresson, 1992; Abdourhamane Touré, 2011; Mamadou, 2012; Robert et al., 2017) as well as anthropogenic activities (soil labor and tillage).

Characterizing the hydrodynamic properties of surface features, in particular hydraulic conductivity, is an essential step in understanding flowing water and solute transport processes in the soil-plant system (Autovino et al., 2018; Basile et al., 2020; Farzamian et al., 2021; Wang et al., 2025). However, hydraulic conductivity measurements are scarce in the Sahel and often concern soil occupations and not their composite elements, i.e., surface features. The aim of the present work is therefore to assess the hydraulic conductivity of six dominant surface features in the Sahel. Specifically, the aim is to determine the impact of soil physical properties on the hydraulic conductivity of surface features and to characterize their implications for soil infiltrability and rainwater runoff.

2. Materials and Methods

2.1. Study Site

The measurements were carried out near the complex of lakes on the eastern and northeastern periphery of the city of Niamey (southwestern Niger) (**Figure 1**). The lakes were Bangou Kirey (13˚29'50" N - 13˚30'49" N and 2˚13'51" E - 2˚13'36" E), Kongou (13˚33'31.07" N - 13˚36'27.04" N and 2˚13'13.37" E - 2˚9'40.30" E), and Bartiawal Kaïna (13˚41'26.9" N - 13˚41'11.0" N and 02˚08'27.7" E - 02˚10'25.0" E), located to the east and northeast of Niamey (Niger), respectively 15 km, 13 km, and 20 km from the city center. These water bodies were formed as a result of hydrological and hydrogeological changes marked by increased runoff and rising water tables (Leduc et al., 2001; Abdourhamane Touré et al., 2016; Maman Aminou et al., 2019; Hado et al., 2021; Moussa Boubacar, 2023). They are part of the chain of water bodies of the Ouallam kori, a fossil tributary of the Niger River. Bangou Kirey and Kongou have been permanent since the early ’60s, and Bartiawal Kaïna since 1986. Bangou Kirey, Kongou, and Bartiawal Kaïna are respectively 1.84 km, 12.2 km, and 40.8 km long and 0.35 km, 0.96 km, and 0.66 km wide (April 2025 measurement). The average water surface areas are 0.4 km^2, 4.62 km^2, and 12.91 km^2, respectively. They therefore exceed the 0.03 km^2 surface limit that qualifies them as lakes (Messager et al., 2016; Pi et al., 2022; Mathilde, 2023). The Bangou Kirey, Kongou, and Bartiawal Kaïna watersheds cover 49 km^2, 149 km^2, and 892 km^2, respectively (**Figure 1**). They are bordered by sandstone plateaus at altitudes ranging from 255 to 267 m. Irrigation is practiced all year round in the immediate vicinity of the lakes, as well as in the bottomlands and low glacis. Rainfed millet and beans are also grown on the glacis, while groundnuts are grown on small wind sails stabilized above the plateaus during the rainy season (June-September).

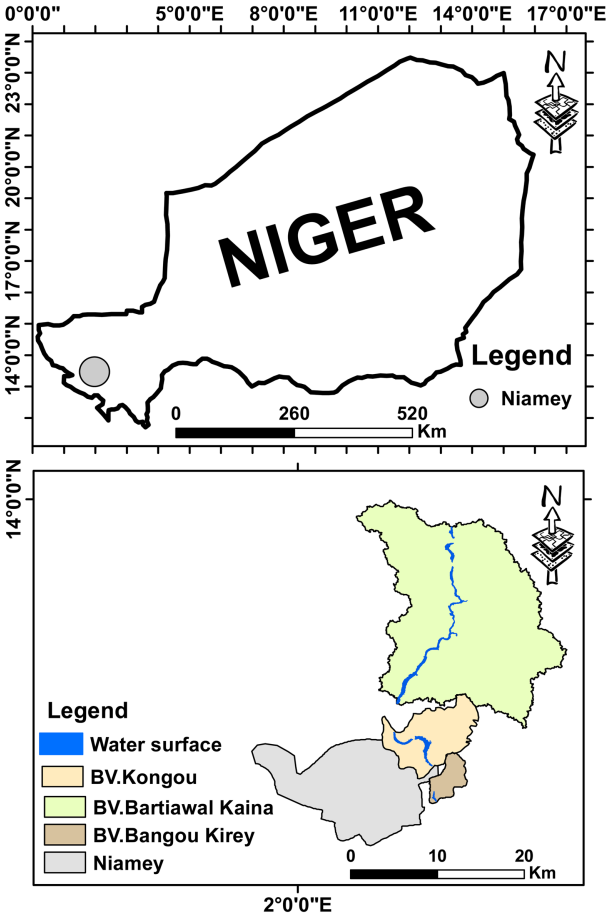

Figure 1. Location of the three contiguous watersheds studied.

2.1.1. Description of Surface Features

The characterization of surface features concerned six (6) different surface features prevailing in the complex of lakes of the eastern-northeastern periphery of the city of Niamey. These were the encrusted surfaces of the plateau (SEP) and glacis (SEG), undegraded surfaces (SND), sown surfaces (SEb), walking paths (PP), and koris bottoms (K).

- Undegraded surfaces (SND): They are located on the lower glacis and are cultivated with millet (**Figure 2(a)**). These surfaces are very heterogeneous and include small areas of erosion crust, bare soil, termite veneers, and manure-covered surfaces. Crop residues are the dominant plant cover in the dry season, and millet and bean plants in the rainy season. They are made up of dune soils with shrubs dominated by *Guiera Senegalensis* and a few *Faidherbia Albida*. The soils are sandy, in the image of Sahelian sandy soils that are naturally poor to very poor in fertilizers and organic carbon (Edahbi et al., 2014; Issa et al., 2020; Idé, 2022; Noma Adamou et al., 2024a). These soils account for over 80% of Niger's agropastoral zone (Gavaud, 1977). Soils on undegraded surfaces were covered by forests during the period 1950-1960 (Sadda et al., 2016; Barmo et al., 2021). For example, more than half of the sandy slopes of Saga Gorou (south of the Ouallam Kori watershed) were covered by forest in 1950

(Abdourhamane Touré et al., 2010). This vegetation was completely cleared in 1975 and put under cultivation (Abdourhamane Touré et al., 2010). One third of the Kori Ouallam watershed was occupied by woody vegetation in 1972 (Noma Adamou et al., 2024b). More than half of this woody vegetation was cleared in favor of cultivated surfaces in 2019 (Noma Adamou et al., 2024b), which are highly susceptible to erosion (Rajot et al., 2009; Abdourhamane Touré et al., 2018; Noma Adamou et al., 2022). The degradation of cultivated surfaces by this erosion leads to the formation of encrusted surfaces not suitable for agriculture.

- Erosion crusts (EC): These develop particularly on soils above plateaus and high glacis (**Figure 2(b)** and **Figure 2(c)**). They form following the removal, by wind and runoff, of loose particles on top of structural crusts (Fan et al., 2008, Neave & Rayburg, 2007; Ran et al., 2012; Yeom, 2017; Bullard et al., 2018). Erosion crusts are made up of a thin, compact, smooth layer due to the smoothing of structural crusts by the repeated impact of raindrops or the stripping of superficial micro-horizons from structural crusts (Casenave & Valentin, 1989; Malam Abdou, 2014). Their formation has been intensified by deforestation and rainfall deficits observed over the decades 1970-1990, which led to the degradation of the Sahelian vegetation cover (Ballouche & Taïbi, 2013; Ozer & Perrin 2014; Kabore et al., 2017; Millogo et al., 2017). Erosion crusts represent an acute level of land degradation (Malam Issa et al., 1999; Habou et al., 2016; Hamadou Younoussa et al., 2018). In the Bangou Kirey, Kongou, and Bartiawal Kaïna watersheds, the crusts on the high glacis are developed on the B horizon after all the A horizon has been eroded and have become unsuitable for cultivation. Those above the plateaus are developed on shallow, undifferentiated soils above lateritic rock.
- Bottom of the koris (K): The "koris" are gullies with highly variable cross-sections ranging from a few decimeters to several tens of meters (Abdourhamane Touré et al., 2010; Alzouma Sanda et al., 2019; Adamou et al., 2023; **Figure 2(d)**). They arise on plateau slopes (Barké et al., 2017). They excavate the glacis and end their trajectory in the bottomlands. They consist of a soft-textured bottom and abrupt banks up to 6 m deep (Mamadou, 2012; Noma Adamou, 2022). Koris can evolve rapidly. For example, between 1996 and 2005, the Gorou Kirey kori (southwest of Niamey) increased from 119 ha to 127 ha (Mamadou, 2012). From 1975 to 2015, in the Kongou watershed, kori lengths increased by an average of 3.72 km (Abdourahamane Touré et al., 2017). Between 2006 and 2008, in Tondi Kiboro (southwest Niger), an average lengthening rate of 4 m yr^{-1} was measured at two (2) koris (Bouzou et al., 2020). The koris carry water and sediment, and also contribute to the silting up of rivers and water bodies (Mamadou, 2012; Tidiane Dia et al., 2023). The Boubon kori, for example, carried around 8,500 tons of sediment and 1,300,000 m^3 of water into the River Niger in 2009 (Mamadou, 2012).
- Irrigated perimeters (Pi): These are found in the bottomlands and on the lower

glacis. Two types of surface feature are mainly observed in irrigated perimeters (**Figure 2(e)**). These are sown surfaces (SEb) and walking paths (PP). These two surface features alternate between hollow areas (SEb) and walking paths (PP). The SEb is, on average, 10 cm deep, 20 - 30 cm wide, and 3 - 20 m long. Cash crops include cereals (sorghum (*sorghum halepense*), maize (*Zea mays*), wheat (*Poacées*)) and legumes (onion *(Allium cepa)*, gumbo (*Abelmoschus esculentus*), bell pepper (*Capsicum annuum*), tomato (*Solanum lycopersicum*), green pepper (*Capsicum frutescens*), lettuce (*Lactuca sativa*), cabbage (*Brassica oleracea*) and carrot (*Daucus carota*)). Irrigation is carried out year-round in irrigated areas. Cultivation practices remain manual, with hoe and hilar tilling. Motor-driven pumps and watering cans are used to water the sown areas (SEb), either directly from the lakes or from the water table via a well. Walking paths are located between the SEb. They are used by irrigators to water their plants. They appear compacted due to trampling.

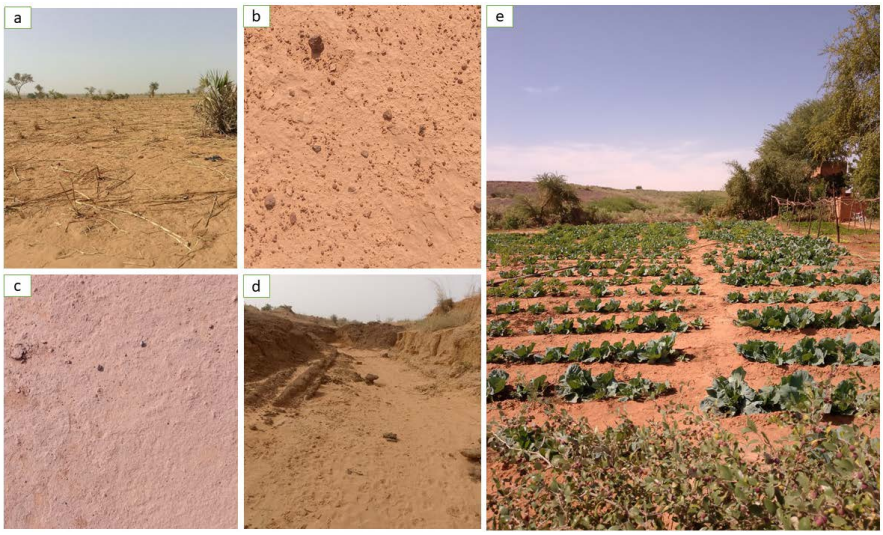

Figure 2. Dominant surface features in the complex of lakes of the eastern-northeastern periphery of Niamey City: a: undegraded surfaces (SND); b: crusted plateau surfaces (SEP); c: crusted glacis surfaces (SEG); d: kori bottoms (K); e: irrigated perimeters (Pi).

2.2. Measuring Hydraulic Conductivity

The BEST method (Beerkan Estimation of Soil Transfer Parameters) is used to carry out infiltration measurements (Di Prima, 2015; Di Prima, et al., 2016; Angulo-Jaramillo et al., 2016; Bagarello et al., 2014, 2017; Fusco et al., 2024). The choice of this method is based on the fact that it is cheaper and more robust than laboratory approaches, which are often costly, tedious, and require specialized equipment—a major constraint for developing countries (Fernández-Gálvez et al., 2019). The principle of the BEST method is based on measuring the infiltration time of a layer of water under constant load infiltrating the soil. The main interest of the test is to enable a comparison of the hydrodynamic behavior of the soil in space and time.

Infiltration measurements were carried out on six (6) surface features of the complex of lakes in the east-northeast periphery of Niamey. These were the encrusted surfaces of the plateaus (SEP) and glacis (SEG), the undegraded surfaces (SND), the sown surfaces (SEb), the walking paths (PP), and the bottoms of the koris (K). Infiltration measurements were carried out using a 10 cm-diameter PVC cylinder manually inserted four centimeters (4 cm) into the soil, minimizing disturbance to the surface (Figure 3). A plastic film was placed on the soil inside the PVC tube to ensure that the pouring of water did not disturb the surface structure and pellicular porosity. A volume of 160 mL of drinking water was then poured onto the plastic film, which was immediately removed while the stopwatch was started to determine the infiltration time of the 160 mL (Figure 4). This exercise was repeated until the soil was saturated. A total of 293 infiltration measurements were carried out (Table 1). The coordinates of each measurement point were taken with a GARMIN GPS and then projected onto the different catchment areas using ArcGIS software (Figure 5). For security reasons, the measurements were based further south in the Bartiawal Kaïna watershed, while they covered around 37 % of each of the Kongou and Bangou Kirey watersheds. The number of measurement points on the six (6) surface features ranged from 21 on crusted plateau surfaces (SEP) to 94 on undegraded surfaces (SND). The greater number of measurements on undegraded surfaces (SND) is explained by their greater heterogeneity. The smaller number of measurement points on the crusted surfaces of the plateaus (SEP) is mainly linked to the duration of infiltration (Table 1).

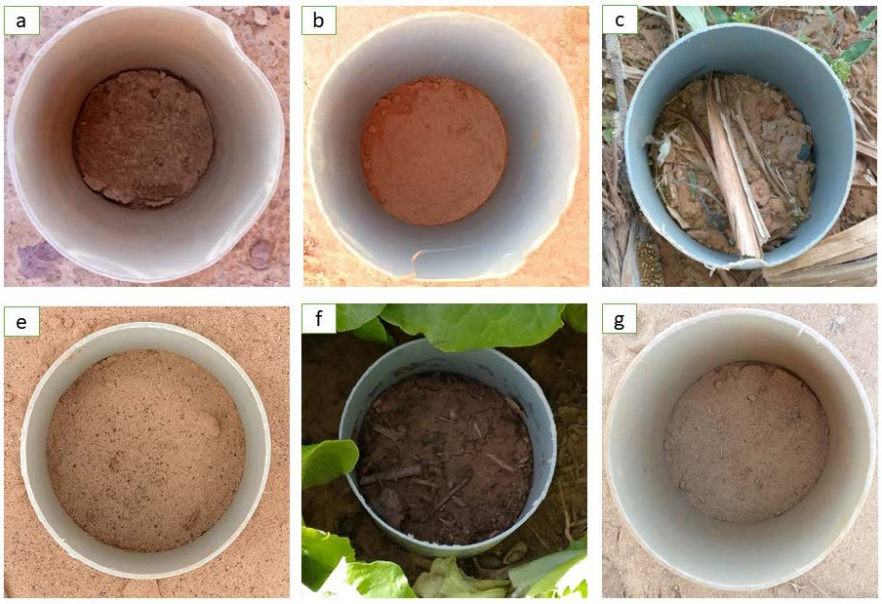

Figure 3. Device for measuring infiltration using the BEST method on six (6) surface features: a) encrusted plateau surfaces (SEP), b) encrusted high glacis surfaces (SEG), c) undegraded surfaces (SND), e) koris bottom (K), f) sown surfaces (SEb), g) walking paths (PP).

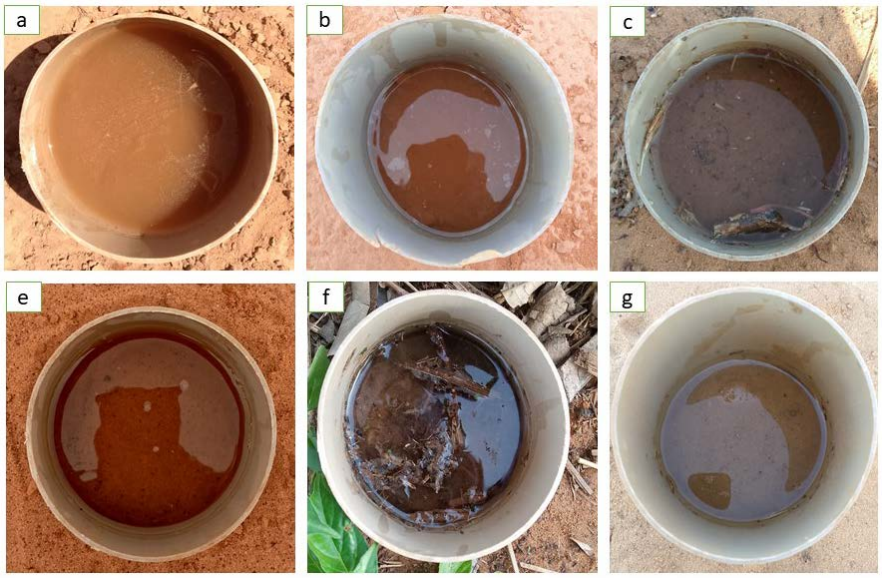

Figure 4. Measurement of water infiltration on the surface features measured: a: encrusted plateau surfaces (SEP), b: encrusted high glacis surfaces (SEG), c: non-degraded surfaces (SND), e: koris bottom (K), f: sown surfaces (SEb), g: walking paths (PP).

Table 1. Distribution of the number of infiltration measurements carried out by surface feature (encrusted plateau surfaces (SEP), encrusted high glacis surfaces (SEG), undegraded surfaces (SND), koris bottom (K), sown surfaces (SEb), walking paths (PP)).

Surface features	SEP	SEG	SND	K	SEb	PP
number of measurements	21	61	94	53	35	29
Mean time per measurement point (S)	2998	852	449	167	697	1152

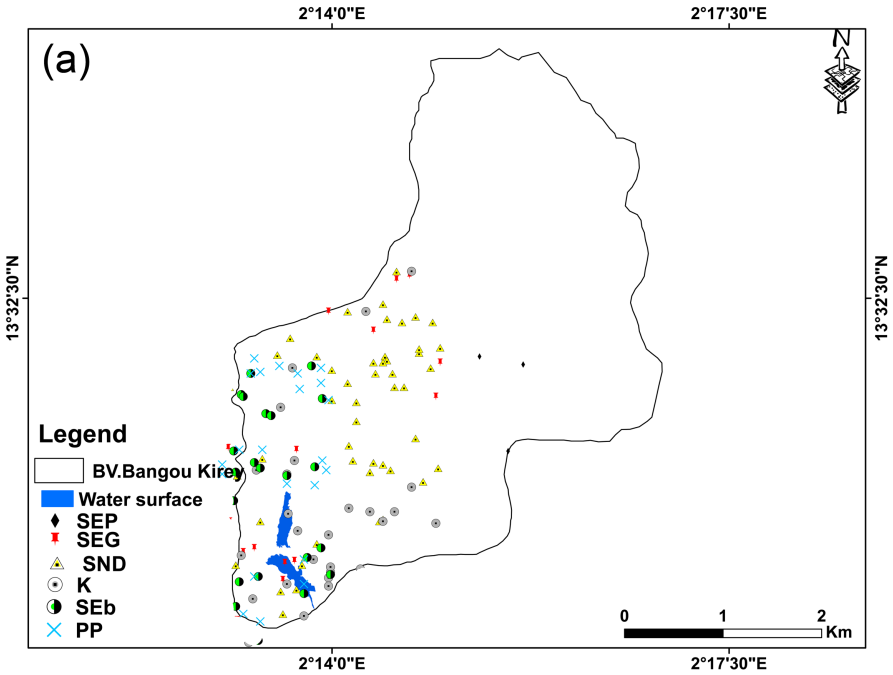

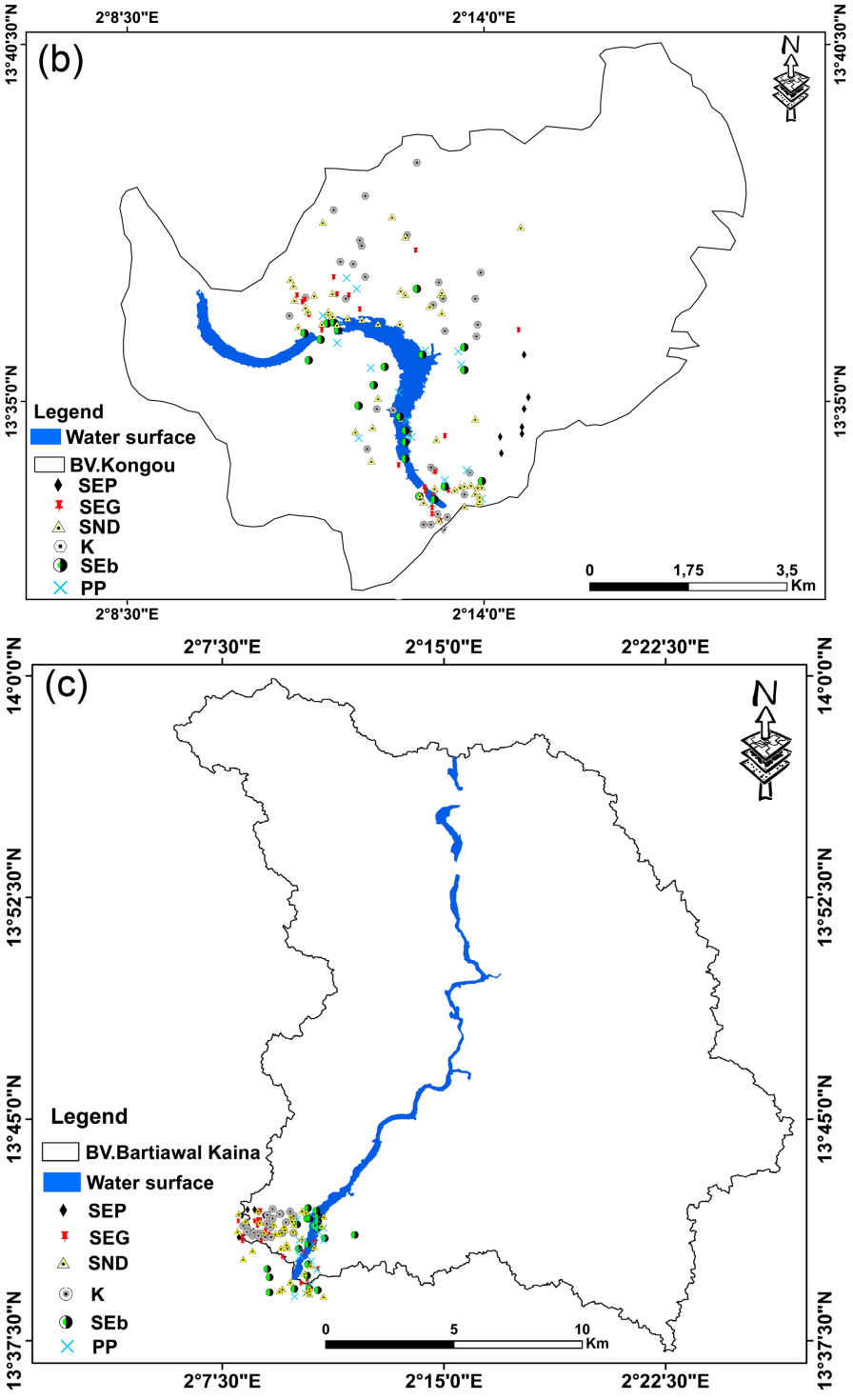

Figure 5. Spatial distribution of hydraulic conductivity measurement points in the catchment areas: (a) Bangou Kirey; (b) Kongou; and (c) Bartiawal Kaïna.

Hydraulic conductivity (Ks) was determined at each measurement point by applying the algorithm developed by Bagarello et al. (2012). This algorithm is based on the calculation of the parameter α (mm^{-1}), which corresponds to a general description of the textural and structural characteristics of the soil (Reynolds & Elrick,

1990; Reynolds & Elrick, 2002; Bagarello et al., 2012; Bagarello & Iovino, 2013). The parameter α expresses the relative importance of gravity and capillarity during the infiltration process (Reynolds & Elrick, 1990; Bagarello et al., 2012). α, which corresponds to the directing coefficient of the infiltration curves, is obtained by linear fitting of the infiltration volume as a function of time (**Figure 6**). A minimum coefficient of determination of 0.80 ($R^2 \geq 0.80$) was considered for each fit (**Figure 6(b)**). Linearity may be unyielding due to cycle perturbation at the start of the infiltration process (Vandervaere et al., 2000; Bagarello et al., 2012). This initial disruption of the infiltration process is due to factors such as hydrophobicity, initial trapping in the soil, or turbulence of applied water volumes (Carrick et al., 2011). It was therefore not always possible to directly obtain the minimum coefficient of determination ($R^2 = 0.80\%$). In 70% of measurements, it was necessary to delete one or two data points, generally the first in the series (**Figure 6**). The determination of α enabled the determination of hydraulic conductivity (Equation 2). The latter is a key parameter for describing the hydrodynamic behavior of soils (Wang et al., 2025).

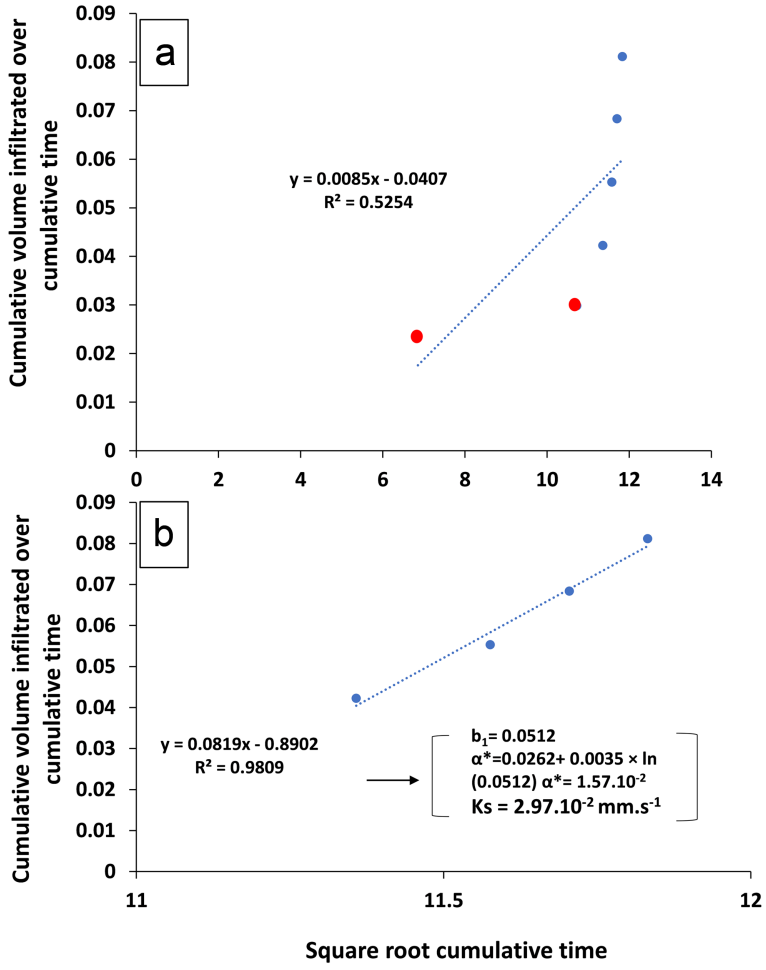

Figure 6. Example of infiltration curves for one measurement: (A) infiltration curve disturbed at the beginning, requiring the elimination of two points in red; (B) perfect curve infiltration (after elimination of the first two points).

$$\alpha^* = 0.0262 + 0.0035 \times \ln(b_1) \quad (1)$$

with b_1 ($L \cdot s^{-1}$), the directing coefficient of an infiltration curve

$$Ks = \frac{b_1}{0.047\left(\frac{2.92}{ra^*} + 1\right)} \quad (2)$$

where Ks ($mm \cdot s^{-1}$) is the hydraulic conductivity and r (mm) is the cylinder radius.

2.3. Determination of Soil Surface Texture and Density

Soil granulometry and pellicular density play a key role in the hydrodynamic behavior of soils (El Mazi et al., 2021). Soil texture and density were then determined using the same soil samples. They were taken from the top five (5) centimeters of soils of different surface features using a 100 cm^3 metal cylinder. The cylinder was manually inserted into the soils of sown surfaces (SEb), undegraded surfaces (SND) and koris bottoms (K). A sledgehammer was used for rigid surfaces, i.e., the encrusted surfaces of plateaus (SEP) and glacis (SEG), and walking paths (PP). Five (5) samples of one hundred cubic centimeters (100 cm^3) each were also taken from each surface feature and packaged in plastic bags. These samples were pre-weighed on a precision balance (accuracy: 10^{-2}) to determine the fresh mass, then dried in an oven at 44˚C for 48 hours. At this temperature, all the water contained in the soil samples was evaporated, and the mass of the samples was stabilized after 48 hours of drying in the oven. Each sample was then weighed to determine the mass of the solids. The determination of these two masses was used to calculate, among other things, the bulk density (Equation 3) and the real density (Equation 4).

$$Da = \frac{Mf}{V} \quad (3)$$

$$Dr = \frac{Ms}{V} \quad (4)$$

where Da: bulk density ($g \cdot cm^{-3}$), Dr: true density ($g \cdot cm^{-3}$), Mf: mass of fresh soil (g), Ms: mass of solids (g), and V: sample volume (cm^3).

Soil texture was determined by the dry sieving method (Seck & Sy, 2021). Each sample was poured into a column of three (3) sieves: 2000 µm, 250 µm, and 63 µm. The three (3) fractions obtained after sieving—mean to very coarse sands, very fine to fine sands, and fine fraction (Clay + Lime)—were weighed on a precision balance (accuracy: 10^{-4}) to determine the mass proportion of each fraction in the first five (5) centimeters of the soils of the different surface features (Equation 5).

$$Fi = \frac{mi}{M} * 100 \quad (5)$$

Fi: mass proportion of fraction i (%); mi: mass of fraction i (g); M: total sample mass (g).

2.4. Determination of Rain Intensity

Rainfall was measured using a 20 mL tipping-bucket rain gauge corresponding to

a 0.5 mm tipping of rain. The rain gauge, which belongs to the AMMA CATCH observatory, was installed in June 2021 at 40 m from Bangou Kirey Lake and 1 m above ground level. The number of tips, the corresponding rainfall height, date, and time are automatically recorded in a datalogger. The tipping time was used to calculate the instantaneous rainfall intensity for each 0.5 mL of rainfall, i.e., 3501 rainfall intensities calculated over the 158 rainfall events recorded between July 2021 and October 2024 (Equation 6). The determination of the 3501 rainfall intensities enabled us to calculate the average and maximum intensities during each rainfall event. Rainfall intensity is a factor that conditions runoff and infiltration of water into the soil (Radcliffe & Simunek, 2010; Darboux et al., 2024). Runoff occurs when rainfall intensity exceeds the soil's infiltration capacity, and infiltration occurs when rainfall intensity falls below the soil's infiltration capacity (Horton, 1933; Bilodeau, 2023; Darboux et al., 2024). The instantaneous rainfall intensities were then compared with the hydraulic conductivities of the surface feature to determine the proportion of rainfall runoff and/or infiltrated into each surface feature during the four seasons of rainfall measurements (Equations 7 and 8).

$$Ip = \frac{Hp}{T} \tag{6}$$

where Ip is the instantaneous rain intensity ($mm{\cdot}s^{-1}$), Hp is the instantaneous rain height (mm), and T is the tipping time (s).

$$R = \frac{ni}{N} * 100 \tag{7}$$

$$I = \frac{n}{N} * 100 \tag{8}$$

where R: proportion of rain that ran off (%); I: proportion of rain that infiltrated (%); ni: number of times $Ip \geq Ks$; n: number of times $Ip \leq Ks$; and N: number of measurements of Ip = 3501.

3. Results

3.1. Hydraulic Conductivity of Surface Features

Hydraulic conductivity varied from one surface feature to another. On average, it varied between 4.6×10^{-2} $mm{\cdot}s^{-1}$ ($\pm 4.6 \times 10^{-2)}$, the highest value measured in the koris, and 9.7.10-4 $mm{\cdot}s^{-1}$ ($\pm 5.1 \times 10^{-4}$), the lowest value determined on the crusted surfaces above the plateaus (**Table 2**). Spatial variability is linked to the dominance of surface features. These are generally spatially distributed according to geomorphological units. Erosion crusts dominate on the plateau (SEP) and the high glacis (SEG), undegraded surfaces (SND) on the low glacis, and irrigated surfaces (SEb and PP) are present in the low glacis and bottomlands (**Figure 7**). From the uplands to the bottomlands, hydraulic conductivity tends to increase. The greatest increase in conductivity occurred in the transition from the crusted surfaces at the top of the plateaus to those in the high glacis, where it fell from 9.7×10^{-4} $mm{\cdot}s^{-1}$ to 7.0×10^{-3} $mm{\cdot}s^{-1,}$ i.e., a 7.3-fold increase. Hydraulic conductivity averaged 1.3×10^{-2} $mm{\cdot}s^{-1}$ ($\pm$ 0.95 $\times 10^{-2}$) on the undegraded surfaces (SND) of the low glacis area, currently

dominated by rainfed millet crops associated with beans. It was of the same order of magnitude as that determined at the level of the sown surfaces (SEb) of the irrigated surfaces and fourteen times higher than that determined on the encrusted surfaces of the plateau (SEP) (Table 2). Conductivity at the bottom of the koris was the highest of all surface features (Table 2). On average, it was 4.6×10^{-2} mm·s^{-1} ($\pm$ 4.6×10^{-2}), more than 3 times higher than that of undegraded surfaces.

Table 2. Hydraulic conductivity measurements on different surface features (encrusted plateau surfaces (SEP), encrusted high glacis surfaces (SEG), undegraded surfaces (SND), koris bottom (K), sown surfaces (SEb), and walking paths (PP)).

Ks (mm·s^{-1})	Surface features					
	SEP	SEG	SND	K	SEb	PP
Min	0.00024996	0.00033396	0.00102614	0.00237915	0.0010355	0.00053931
Max	0.00189646	0.02013348	0.04863784	0.24170982	0.09485938	0.04442209
Mean	0.00097767	0.00703417	0.0133647	0.04698576	0.01600034	0.00732445
Median	0.00093218	0.00650281	0.01120474	0.03038166	0.00678376	0.00447626
Ecartype	0.00051752	0.00519639	0.00955681	0.04600551	0.02214397	0.00970502
CV (%)	52.9341261	73.8734425	71.5079025	97.9137266	138.396893	132.50162
number of measurements	21	61	94	53	35	29

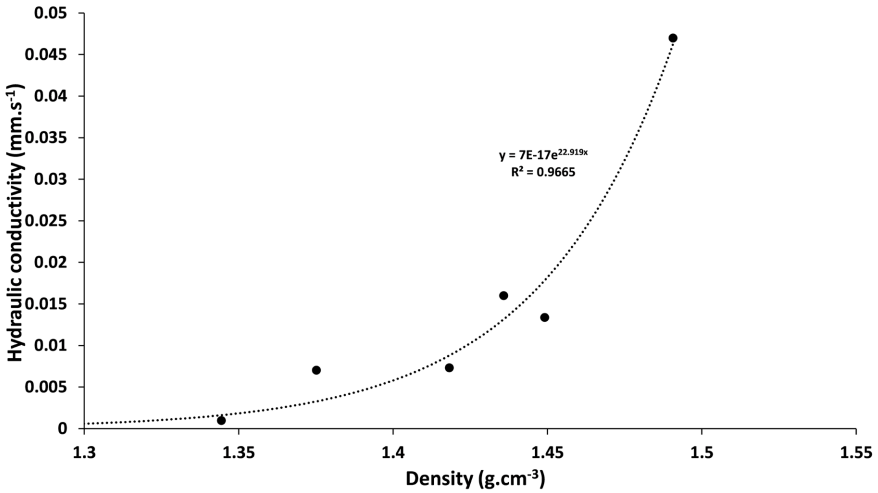

Figure 7. Variation of hydraulic conductivity as a function of density for different surface features.

Hydraulic conductivity showed no significant difference ($P = 0.05$) for the same surface feature in all three (3) contiguous catchments, Bartiawal Kaïna, Bangou Kirey, and Kongou (Table 3). Hydraulic conductivity, however, was characterized by a strong dispersion of the mean values obtained on each of the six surface features. The dispersion of hydraulic conductivity was very high on sown surfaces (SEb) and walking paths (PP), with coefficients of variation of 138.39 and 132.50%,

respectively (Table 3). It was relatively low on encrusted plateau surfaces (SEP) (CV = 53%), encrusted glacis surfaces (SEG) (CV = 74%), undegraded surfaces (SND) (CV = 71%), and kori bottoms (K) (CV = 98%).

Table 3. ANOVA test among surface features of watersheds (encrusted plateau surfaces (SEP), encrusted high glacis surfaces (SEG), undegraded surfaces (SND), koris bottom (K), sown surfaces (SEb), walking paths (PP)).

TEST ANOVA ($P = 0.05$)	Surface features					
	SEP	SEG	SND	K	SEb	PP
Bangou Kirey	$(0.000686)_a$	$(0.006517)_b$	$(0.011356)_c$	$(0.035418)_e$	$(0.013192)_h$	$(0.004324)_i$
Kongou	$(0.000981)_a$	$(0.006164)_b$	$(0.010996)_c$	$(0.057625)_e$	$(0.009708)_h$	$(0.003415)_i$
Bartiawal Kaïna	$(0.001264)_a$	$(0.008164)_b$	$(0.016561)_c$	$(0.052205)_e$	$(0.020408)_h$	$(0.011366)_i$

3.2. Variation in Texture and Density of Different Surface Features

Soil surface density was almost similar across the six surface features studied (Table 4). It ranged from 1.31285 g·cm^{-3} in the crusted surfaces of the haut-glacis (SEG) to 1.49064 g·cm^{-3} in the koris (Table 4). However, in absolute terms, average density varies according to topography. It tends to increase from plateau to bottomlands. Hydraulic conductivity increases exponentially with soil density (Figure 7). The highest (4.6×10^{-2} mm·s^{-1} ± 4.6×10^{-2}) and lowest (9.7×10^{-4} mm·s^{-1} ± 5.1×10^{-4}) hydraulic conductivities corresponded, for example, to the highest and lowest densities determined in the koris (K) and plateau crusted surfaces (SEP), respectively.

Table 4. Density of surface features (encrusted plateau surfaces (SEP), encrusted high glacis surfaces (SEG), undegraded surfaces (SND), kori bottom (K), sown surfaces (SEb), and walking paths (PP)).

Density (g·cm^{-3})	Surface features					
	SEP	SEG	SND	K	SEb	PP
Mean	1.3444	1.31285	1.44914	1.49064	1.43582	1.41822
Ecartype	0.12634	0.05737	0.07311	0.08759	0.09620	0.14113

The soils of the different surface features are dominated by the sandy fraction, whose content ranged from 95% on the crusted surfaces of the plateaus to almost 100% in the koris (K) as shown in Table 5. The mean to very coarse sand fraction dominated all surface features, with contents ranging from 50% on the crusted surfaces of the plateaus to 68% in the koris. This fraction is followed by very fine to fine sands, with contents ranging from 31% in the koris to 46% in the encrusted surfaces of the high glacis. The fine silty-clay fraction reaches a maximum of 4.62% in the crusted surfaces of the plateaus. The kori bottoms have the lowest fine fraction content (0.17%). The particle size distribution of the different surface features appears to vary according to topography. Mean to very coarse sands tend to increase from plateaus to bottomlands, while the fine fraction (clay + silt) varies in

the opposite direction.

Table 5. Granulometric distribution of surface features at the soil surface (encrusted plateau surfaces (SEP), encrusted high glacis surfaces (SEG), undegraded surfaces (SND), Koris bottom (K), sown surfaces (SEb), walking paths (PP)).

Particule size class	Surface features					
	SEP	SEG	SND	K	SEb	PP
Mean to very coarse sand (%)	50.22	51.20	51.68	68.16	55.57	57.51
Very fine to fine sand (%)	45.14	46.64	46.41	31.65	42.66	40.86
Clay+ Silt (%)	4.62	2.15	1.89	0.17	1.75	1.62

Hydraulic conductivity showed a difference according to the different particle-size fractions of the soils in the different surface features. It tends to increase as the fraction of mean to very coarse sands increases and tends to decrease as the fraction of very fine to fine sands increases or as the clay-loam fraction increases. This decrease is particularly significant as the fine fraction (A + L) increases. Increasing the fine fraction causes at least a four (4)-fold reduction in hydraulic conductivity than that induced by very fine to fine sands (Figure 8).

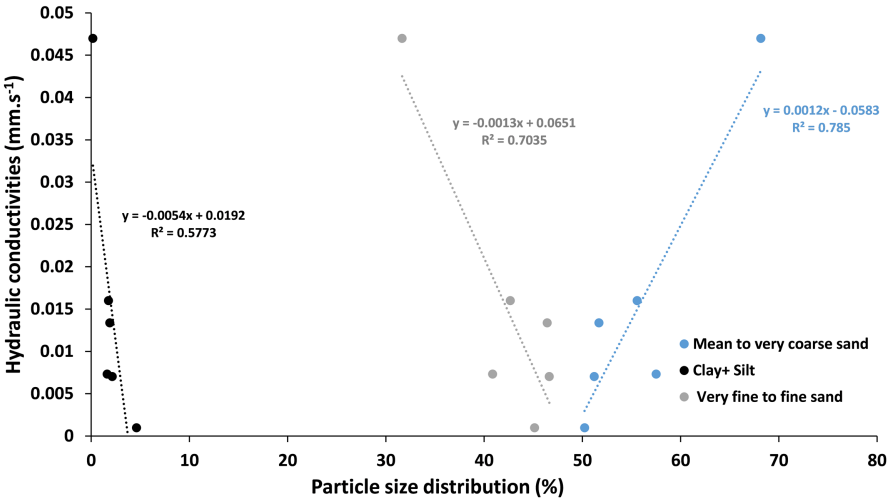

Figure 8. Variation in hydraulic conductivity according to the content of different particle-size fractions.

3.3. Variation of Rainfall Intensity

One hundred and fifty-eight (158) rainfall events were recorded between July 10, 2021, and October 06, 2024. 3501 instantaneous intensities were then calculated after each tipping of the bucket. The maximum intensity during the one hundred and fifty-eight (158) events varied between 1.39×10^{-5} and 0.25 mm·s^{-1} for the rainfall recorded (Figure 9). It was high ($Ip \geq 0.05$ mm·s^{-1}) on only five (5) occasions. High-intensity rainfall had a probability of occurrence of 3.16% and was recorded between July and September (Table 6). One hundred and

twenty-five (125) maximum rainfall event intensities were low ($Ip \leq 0.025$ mm·s^{-1}), and twenty-eight (28) were intermediate, i.e., between 0.025 mm·s^{-1} and 0.05 mm·s^{-1}, with respective probabilities of occurrence of 79.11% and 17.72%. These cases were recorded between July and August in 64.28% and 70% of cases, respectively.

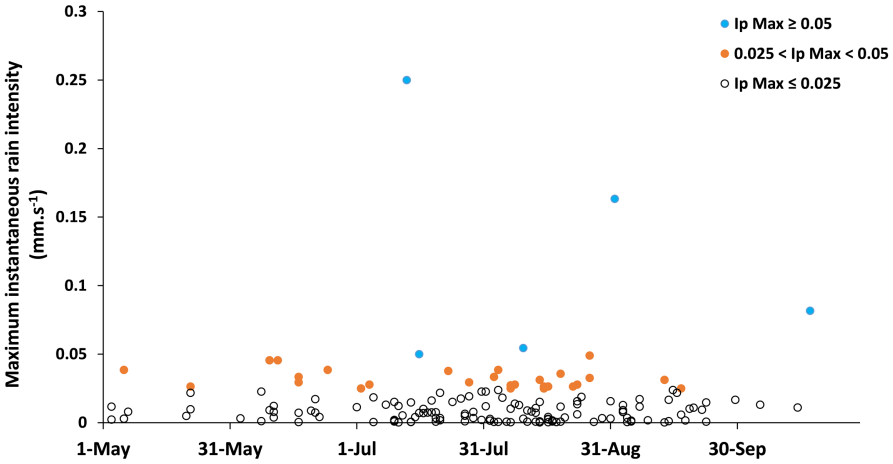

Figure 9. Variation in maximum intensity of recorded rainfall events between 2021 and 2024.

Table 6. Probability of occurrence of *Ip* Max for the 158 rainfall events in each maximum-intensity interval.

Ip Max for the 158 rainfall events interval (mm·s^{-1})	*Ip* Max ≥ 0.05	0.025 < *Ip* Max < 0.05	*Ip* Max ≤ 0.025
Class Numbers (n)	5	28	125
Probability of occurrence (%)	3.16	17.72	79.11

During a rainfall event, the instantaneous intensity of rainfall is highly variable, forming a unimodal form in 96.2% of cases and two (2) to six modes in 3.8% of cases. Instantaneous intensity increases rapidly at the start of the rain event, peaking on average 700 seconds (12 minutes) after the rain begins (Figure 10). It then falls slowly for around 2375 seconds (40 minutes), ending with streaks that can last up to 4000 seconds. From 2021 to 2024, a rain event lasts an average of 2074 seconds (35 minutes) for an average intensity of 7.3×10^{-3} ($\pm 8.5 \times 10^{-3}$) mm·s^{-1}.

Of the 3501 measurements, the instantaneous rainfall intensity was 89.09% greater than the hydraulic conductivity determined on the crusted surfaces of the plateaus (SEP), whereas in the koris this percentage was only 0.57% (Table 7). This means that 89.09% of the rain falling on the crusted plateau surfaces (SEP) would run off, while the rainwater would be more likely to infiltrate the koris. On the encrusted surfaces of the high glacis (SEG) and walking paths (PP), the instantaneous rainfall intensities were regularly higher than the hydraulic conductivity. These surfaces would generate runoff in 59.53% of cases. These proportions are 37.71% and 26.57% for undegraded surfaces (SND) and sown surfaces (SEb), respectively.

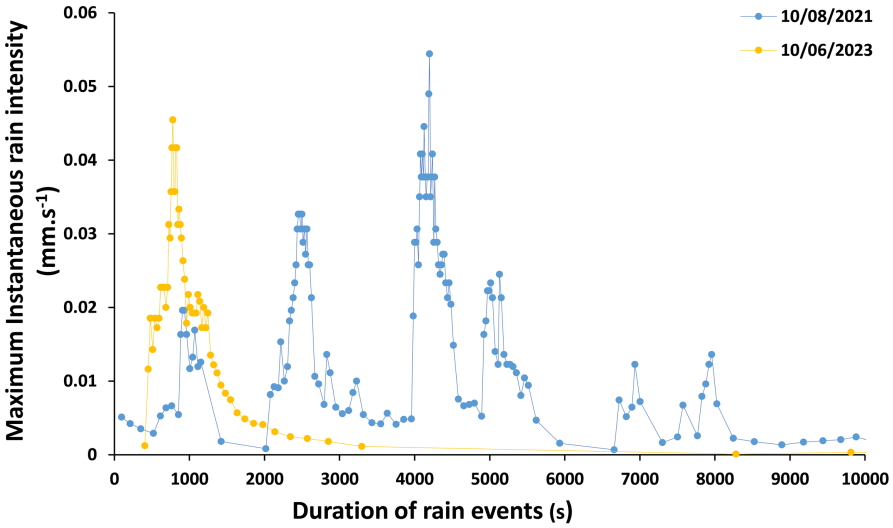

Figure 10. Types of rainfall intensity variation during two (2) rain events.

Table 7. Variation in the probability of runoff occurrence on different surface features.

Ip	Surface features					
	SEP	SEG	SND	K	SEb	PP
Number of times $Ip \geq Ks$ (n)	3115	2120	1220	15	934	2091
Rainwater runoff probability	89.09	59.95	37.71	0.57	26.57	59.11

4. Discussion

Although this study spans only four years of measurements, it has allowed the highlighting of the main properties of surface features in the South West Niger area impacting hydraulic conductivity, which play a major role in soil erosion and runoff processes.

Surface features are highly variable in the complex of lakes in the eastern, north-eastern peripheries of Niamey. Their spatiotemporal variability is highly characteristic of Sahelian landscapes, which are composed of a diversity of land cover units, the most important being millet fields, irrigated perimeters, and degraded surfaces. The surface features that make up these units are, in particular, the encrusted surfaces of the plateaus (SEP) and the high glacis (SEG), the undegraded surfaces (SND), the koris bottoms (K), the sown surfaces (SEb), and the walking paths (PP). Organic matter can play a role in the formation and diversity of surface features. However, its low or very low content in Sahelian sandy soils (<1%) means that it plays a negligible role in the formation of surface features (Edahbi et al., 2014; Issa et al., 2020; Idé, 2022; Noma Adamou et al., 2024a). The variability of surface features could be controlled by density, granulometry, soil structure, climate, and human activity (Ben-Hur et al., 2009; Rabouli, 2022; Lin et al., 2025).

The density of the first centimeters of soil was of the same order of magnitude, on average, in the soils of the six (6) surface features studied. It ranged from 1.31

g·cm^{-3} in the crusted surfaces of the haut-glacis (SEG) to 1.49 g·cm^{-3} in the koris. The low variation in density is probably due to the fact that these soils have the same origins and are essentially formerly stabilized dunes (Gavaud, 1968). Density was measured on several soil types in the Sahel (Adefague Mbouryang et al., 2022; Traore et al., 2024). It was 1.25 g.m^{-3} in the cultivated soils of the dune cordon in southwestern Niger (Idé, 2022). In terms of use, these soils are comparable to undegraded surfaces (SND), where the density was slightly higher (1.44 g.m^{-3}). The density of the undegraded surface was identical to that determined on cultivated sandy soils on glacis in the Tougou watershed (North Burkina Faso) (1.44 g.m^{-3}) (Mounirou, 2012). However, the density was higher (1.70 g.m^{-3}) on the crusted surfaces of the Tougou watershed compared with that determined on the plateau (SEP) and glacis (SEG) crusts in this work. This difference could be linked to organic matter content and/or soil porosity. Despite its low variation, density seems to show spatial variability according to topography. The lowest densities were obtained on the crusted surfaces of the plateaus and the highest in the valley interior.

Soil particle size distribution shows that the fraction of mean to very coarse sands dominates in all surface features. It ranged from 50.22% in the crusted surfaces on the plateau (SEP) to 68.16% in the koris (K). Overall, the sandy fraction dominated in all surface features, ranging from 95% in the crusted surfaces of the plateaus (SEP) to almost 100% in the koris (K). The sandy texture of the soils in the six (6) surface features is most probably linked to the fact that they developed on stabilized dunes of aeolian origin (Gavaud, 1977; Niang et al., 2004). Coarse-textured soils are widespread in the Sahel, in both dune and lateritic soils. On dune soils, for example in southern Niger, the sandy fraction varied from 95% (Idé, 2022) to 78.80% (Bationo et al., 2015). Lateritic soils, most often developed above plateaus, reached sand contents of 75% in Burkina Faso (Bassole et al., 2023), 73.66% in Niger (Halidou et al., 2020), and 78.25% in North Cameroon (Adefague Mbouryang et al., 2022). The fraction of mean to very coarse sands also showed a spatial variability similar to that of density. The content of the silty-clay fraction ranged from 4.62% in the crusted surfaces of the plateaus (SEP) to 0.17% in the koris (K). A high clay-loam fraction was found on lateritic soils of the plateau in Kollo, Niger, where it reached 26.34% (Halidou et al., 2020), six (6) times that of the crusted upland surfaces (SEP) of the complex of lakes of the eastern-north-eastern peripheries of Niamey. Similarly, in North Cameroon, the clay-loam fraction reached 21.75% on soils developed above the plateau (Adefague Mbouryang et al., 2022). Spatially, the silty-clay fraction follows an inverse spatial trend relative to that of density and mean to very coarse sands.

The dispersion of hydraulic conductivity was significant across the six (6) surface features. The coefficients of variation were very high in the sown areas (SEb) and the walking paths (PP) of the irrigated perimeters, at 138.39 and 132.50%, respectively. This high dispersion is linked to the diversity of farming tools, cultivation practices, watering levels, and crops cultivated. Dispersion was lower on

crusted surfaces of the plateau (SEP; CV = 52.93%). These surfaces are smooth and bare (Alzouma Sanda et al., 2019). They have the same structure as the glacis encrusted surfaces (SEG), where the relatively higher dispersion averages at 73.87%. The difference in the dispersion of the erosion crusts could then be linked to the nature of their substrates: the crusted surfaces of the plateaus are developed on a lateritic soil, whereas the substrate of the crusted surfaces of the glacis is a sandy soil. Over the entire glacis, both high and low, dispersion was intermediate, most probably due to the fact that the sandy soils had the same aeolian origin (Gavaud, 1968; Niang et al., 2004). Conductivity dispersion (CV = 97.91%) was high at the bottom of the koris.

Hydraulic conductivity was lower on the encrusted plateau surfaces (SEP), 9.7 $\times 10^{-4}$ mm·s^{-1} ± 5.1 $\times 10^{-4}$, i.e., 7 times lower than on the encrusted glacis surfaces (SEG). This is most probably due to the difference in their substrates. Erosional crusts are widespread throughout the world. Their low hydraulic conductivity has been observed in Burkina Faso (Mounirou, 2012), France (Chahinian et al., 2006), Israel (Carmi & Berliner, 2008), Belgium (Lin et al., 2025), and Tunisia (Albergel & Alali, 2003). For example, the hydraulic conductivity measured on glacis encrusted surfaces (SEG), 7.0 $\times 10^{-3}$ mm·s^{-1} ± 5.1 $\times 10^{-3}$, was slightly higher than that determined on glacis crusts (4.4 $\times 10^{-3}$ mm·s^{-1}) in northern Burkina Faso (Mounirou, 2012) and lower than that determined (9 $\times 10^{-3}$ mm·s^{-1}) in Tunisia (Albergel & Alali, 2003). These differences can be explained by measurement techniques (Mrabet et al., 2010), the aggressiveness of rainfall, or the nature of the soil.

Measurements in a five- to seven-year-old fallow in Niger revealed hydraulic conductivities of 5.8 $\times 10^{-3}$ mm·s^{-1} ± 2.5 $\times 10^{-3}$ (Malam Abdou, 2016), which are very similar to those of the encrusted glacis surfaces (7.0 $\times 10^{-3}$ mm·s^{-1} ± 5.1 $\times 10^{-3}$). Old fallows in the Sahel, despite the abundant vegetation cover, increased organic matter content, and biological activity that structure their soils, have crusted soils that reduce their infiltrability (Lavelle et al., 1998; Morsli et al., 2004; Coq et al., 2007; Ngo et al., 2011). It should be remembered that the presence of litter promotes soil infiltrability through the development of aggregates and pores, and termite activities that could improve soil porosity (Ambouta et al., 1996; Leonard & Rajot, 2000; Kaiser et al., 2017).

Hydraulic conductivity was of the same order of magnitude on undegraded surfaces (1.3 $\times 10^{-2}$ mm·s^{-1} ± 9.5 $\times 10^{-3}$ mm·s^{-1}) and on sown surfaces of irrigated perimeters (1.6 $\times 10^{-2}$ mm·s^{-1}; 2.2 $\times 10^{-2}$ mm·s^{-1}). Tilling these surfaces, in fact, creates the porosity that improves hydraulic conductivity. In fact, weeding and hoeing of cultivated surfaces destroy surface crusts and improve soil porosity (Mvondo-Awono et al., 2013). Hydraulic conductivities ranging from 8.3 $\times 10^{-3}$ mm·s^{-1} to 9.1 $\times 10^{-3}$ mm·s^{-1} have been measured in cultivated sandy soils in northern Burkina Faso (Mounirou, 2012). These values were of the same order of magnitude as those for undegraded (SND) rainfed cultivated and irrigated (SEb) surfaces. This is probably due to the fact that these sandy soils are tilled.

Hydraulic conductivity measured at the bottom of the koris was the highest (4.6

$\times 10^{-2}$ mm $s^{-1} \pm 4.6 \times 10^{-2}$). These ubiquitous gullies in the Sahelian landscape are expanding in density, length, width, and depth (Leblanc et al., 2007; Abdourhamane Touré et al., 2017).

Hydraulic conductivity was characterized by very marked spatial variability, not only according to surface features but also according to relief units, as shown in **Figure 11**. It shows the same spatial variability as the fraction of mean to very coarse sands and density (**Figure 7**). In fact, hydraulic conductivity increases exponentially with density. This dynamic is the exact opposite of that observed in compacted cultivated soils in Ukraine (Håkansson & Medvedev, 1995). Hydraulic conductivity increases with the coarse fraction, confirming laboratory tests that have shown that hydraulic conductivity is increased two (2) times in sandy fractions relative to clay samples (Knödel et al., 2007). Increasing contents of very fine to fine sands or silty clay fractions tend to decrease hydraulic conductivity in soils. In Belgium, for example, the high content of the clay-loam fraction (82.6%) lowered hydraulic conductivity by 10% relative to sandy soil (Lin et al., 2025). A downward trend in hydraulic conductivity as the fine fraction increases has been observed in sandy soils in South Africa (Medinski et al., 2009) and Tunisia (Albergel & Alali, 2003).

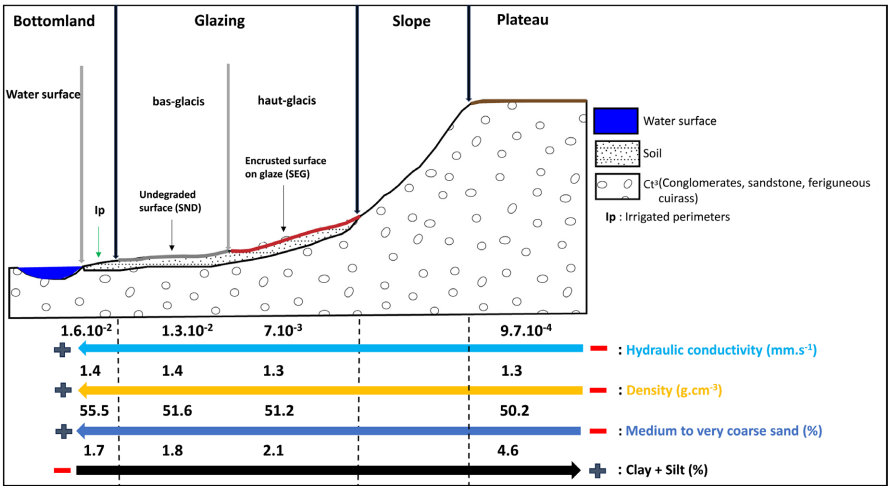

Figure 11. Spatial variation of hydraulic conductivity, density, and granulometry according to topography.

The average rainfall intensity over the four (4) years of measurement was 1.1×10^{-2} mm·s^{-1} ($\pm 10^{-2}$). This value is lower than that determined at the Sahel scale (2.3×10^{-2} mm·s^{-1}) over the period from 1990 to 2015 (Panthou et al., 2018). The maximum instantaneous intensity in the complex of lakes of the eastern-northeastern Niamey periphery was variable from year to year. The short duration of observation, however, did not allow confirmation of the increase in rainfall intensities determined in the Sahel from 1980 onwards (Giannini et al., 2013; Panthou et al., 2014; Sanogo et al., 2015; Panthou et al., 2018).

Rainfall intensity is a determining factor in rainfall runoff. Even if, at the land-

scape scale, watershed runoff is dependent on slope, vegetation cover, and land management practices, runoff generation is driven by rainfall, and it occurs when rainfall intensity exceeds the infiltration capacity of the soil (Horton, 1933; Roose, 1999; Bilodeau, 2023; Darboux et al., 2024).

Surface features showed different hydraulic conductivities, reflecting different runoff rates when rainfall intensity exceeded their hydraulic conductivities ($Ip > Ks$). Runoff was particularly high on encrusted surfaces in 89.09% (SEP) and 59.95% (SEG) of the 3501 measurements where rainfall intensity was higher than hydraulic conductivity. The runoff rate on glacis erosion crusts (59.95%) is within the range of runoff coefficients determined on this type of surface, which have varied in Niger between 60% in Fakara (Descroix et al., 2012) and 98% in the Boubon watershed (Mamadou, 2012).

On undegraded areas cultivated with millet and irrigated perimeters, the runoff rates would be 37.71% and 26.57%, respectively. Even so, the low runoff on the sandy soils widely cultivated in the Sahel could result in land losses through erosion. Erosion by runoff leads to land losses of 1.54 $t{\cdot}ha^{-1}{\cdot}yr^{-1}$ or even 1.92 $t{\cdot}ha^{-1}{\cdot}yr^{-1}$ in Sahelian watersheds (Descroix et al., 2012; Noma Adamou et al., 2022).

The highest hydraulic conductivity was measured at the bottom of the koris, at 4.6×10^{-2} $mm{\cdot}s^{-1} \pm 4.6 \times 10^{-2}$. If rain fell directly on these surfaces, 99.43% would infiltrate (Ks > in 99.43% of cases of 3501 *Ip* measurements). However, as soon as the rainfall is sufficient, at 5 mm (Lubès-Niel et al., 2001; Mamadou, 2012) or even more than 20 mm (Lubès-Niel et al., 2001), the water can run off. The presence of a layer of water during and after the rainfall event, combined with the very high hydraulic conductivity of the bottoms of the koris, could lead to significant infiltration and therefore potential groundwater recharge. The role of koris in groundwater recharge and its rise by several meters in recent decades has been hypothesized, for example, in the Niamey region (Favreau, 2000; Leduc et al., 2001; Abdourhamane Touré et al., 2016; Maman Aminou et al., 2019; Hado et al., 2021; Moussa Boubacar, 2023).

The infiltrability of the surface features prevailing in the complex of lakes of the eastern-northeastern Niamey periphery often exceeds the instantaneous rainfall intensity, which could contribute to soil erosion. To reduce the problem of soil losses through erosion, anti-erosion devices are built, particularly on plateaus, where benches are often constructed (Malam Abdou, 2014; Fiorillo et al., 2017; Noma Adamou, 2022). These structures store a lot of water on plateaus where soils have very low hydraulic conductivity. The very high average potential evapotranspiration in Niamey (9.2×10^{-5} $mm{\cdot}s^{-1}$; Maman Aminou, 2023) suggests that bench-type devices on plateaus would make more water available for evaporation. This would lead to full water losses. The appropriate restoration techniques would be those that slow down the flow rates, similar to stony bands that reduce the risks of runoff and soil loss (Robert, 2011; Khelifa et al., 2017; Xu et al., 2018; Zouré et al., 2019; Jiang et al., 2020; Martínez-Mena et al., 2020).

Intensified cropping and overgrazing lead to extensive land degradation in the

Sahel (Descroix & Nouvelot, 1997; El Bakkari, 2025). In Niger, for example, more than 100,000 ha are degraded every year, marking a large expansion of encrusted surfaces (Folega et al., 2019; Mahamadou et al., 2023; Mahamadou Moudi et al., 2024). It has been shown here that these surfaces allow almost 90% of the rain that falls on them to run off. This percentage could worsen as rainfall intensities have been increasing in the Sahel since 1980 (Panthou et al., 2018). Crusts collect rainfall for koris, where runoff is concentrated (Fiorillo et al., 2017). It should be remembered that koris with very high hydraulic conductivity (4.6×10^{-2} mm·s^{-1} ± 4.6×10^{-2}) are increasing in number, density, and length (Leblanc et al., 2007; Abdourhamane Touré et al., 2017). All of these would suggest a significant increase in the transfer of water flow to groundwater and a further rise in the water table.

5. Conclusion

The aim of this study was to evaluate the hydraulic conductivity of six (6) dominant surface features in the Sahel. The surface features are characterized by great diversity. They include the crusted surfaces of plateaus (SEP) and glacis (SEG), undegraded surfaces (SND), sown surfaces (SEb), walking paths (PP), and koris bottoms (K). These surface features show a zonal distribution according to relief. Indeed, the encrusted surfaces of the plateaus (SEP) and glacis (SEG) develop at higher altitudes, while the undegraded surfaces (SND), sown surfaces (SEb), and walking paths (PP) are mainly found in the lower glacis and bottomlands. Granulometry revealed that the coarse fraction dominated in all surface features, with rates ranging from 95.36% in the encrusted surfaces of the plateaus (SEP) to almost 100% at the bottom of the koris. Density increased from plateau to bottomlands. It ranged from 1.31 g·cm^{-3} in the encrusted surfaces of the high glacis (SEG) to 1.49 g·cm^{-3} in the koris. Increasing the density and fraction of mean to very coarse sands tends to increase hydraulic conductivity, while increasing the fraction of very fine to fine sands, and particularly the clay-loam fraction, decreases hydraulic conductivity. Hydraulic conductivity was highly variable across the different surface features. The highest hydraulic conductivity was measured in the koris (K) (4.6×10^{-2} mm·s^{-1} ± 4.6×10^{-2}). The lowest hydraulic conductivity was obtained on the encrusted surfaces of the plateaus (SEP) (9.7×10^{-4} mm·s^{-1} ± 5.1×10^{-4}), i.e., almost forty-eight (48) times lower than that of the koris. On encrusted plateaus, bench-type or half-moon structures is built. Average potential evapotranspiration is very high in Niamey (9.2×10^{-5} mm·s^{-1}). These structures would therefore make more water available for evaporation. For effective management, it would be more appropriate to construct devices that do not store water but increase hydraulic conductivity and slow down flows over plateaus.

Acknowledgements

This work was supported by FARSIT/MESRIT Project GEPAAP (ÉCOSYSTÈMES DES LACS MERIDIONAUX AU NIGER: Géodynamique, Erosion, Pollution,

Agriculture et Autonomisation des Populations).

Conflicts of Interest

The authors declare no conflicts of interest regarding the publication of this paper.

References

Abdourhamane Touré, A. (2011). *Erosion en milieu sableux cultivé au Niger dynamique actuelle et récente en liaison avec la pression anthropique et les changements climatiques.* Master's Thesis, Université de Bourgogne et Université Abdou Moumouni Niamey.

Abdourhamane Touré, A., Guillon, R., Garba, Z., Rajot, J. L., Petit, C. et al. (2010). Evolution des paysages Sahéliennes au cours des six dernières décennies dans la région de Niamey: De la disparition de la brousse tigrée à l'encroutement de surface des sols. *Pangea Infos, 47,* 35-40.

Abdourhamane Touré, A., Issaka, A. M., Hassane, B., Djibrilla, A. M., & Garba, Z. (2017). Dynamique spatio-Temporelle du ravinement dans le bassin versant du lac Kongou, sud-ouest Niger. *Revue Ivoirienne des Sciences et Technologie, 29,* 181-192.

Abdourhamane Touré, A., Rajot, J. L., Garba, Z., Marticorena, B., Petit, C., & Sebag, D. (2011). Impact of Very Low Crop Residues Cover on Wind Erosion in the Sahel. *CATENA, 85,* 205-214. https://doi.org/10.1016/j.catena.2011.01.002

Abdourhamane Touré, A., Tidjani, A. D., Rajot, J., Bouet, C., Garba, Z., Marticorena, B. et al. (2018). Quantification des flux d'érosion éolienne au cours d'une transition champ-jachère au Sahel (Banizoumbou, Niger). *Physio-Géo, 12,* 125-142. https://doi.org/10.4000/physio-geo.6287

Abdourhamane Touré, A., Tidjani, A., Guillon, R., Rajot, J. L., Petit, C. et al. (2016). Teneur en matières en suspension des lacs sahéliens en liaison avec les variations piézométrique et pluviométrique: Cas des lacs Bangou Kirey et Bangou Bi, Sud-Ouest Niger. *Afrique Science. Revue internationale des sciences et technologies, 12,* 384-392.

Adamou, A., Abdou, K. D., Mounir, Z. M., & Abdoul Kader, S. M. (2023). Les carrières dans le tissu urbain de la ville de Zinder (Niger): Quels enjeux dans la planification urbaine? *Geo-Eco-Trop, 46,* 217-229.

Adefague Mbouryang, C., Basga, S. D., & Doua, S. A. (2022). Dégradations des sols et baisse de la production agricole dans l'arrondissement de Lagdo: Cas du terroir de Djalingo-Kapsiki, Nord-Cameroun. *Afrique Science, 21,* 56-69. http://www.afriquescience.net

Albergel, M. J., & Alali, M. Y. (2003). *Paramètres hydriques des sols dans un aménagement en banquettes anti-érosives (El Gouazine, Tunisie)* (p. 66). Mémoire de D.E.A de l'Université Montpellier II.

Alzouma Sanda, R., Mamadou, I., & Yero, K. S. (2019). Impacts des aménagements antiérosifs sur les ravinements issus de deux plateaux du bassin versant de Boubon au Niger. *Revue Ivoirienne des Sciences et Technologie, 34,* 421-436. http://www.revist.ci

Ambouta, J. M. K. (2007). Ressources en sols; gestion et conservation des sols. In *Compte rendu de conference* (p. 41). FLSH, UAM.

Ambouta, J. M. K., Valentin, C., & Laverdière, M. R. (1996). Jachères et croutes d'érosion au Sahel. *Revue sécheresse, 7,* 269-275.

Amogu, O. (2009). *La dégradation des espaces Sahéliens et ses conséquences sur l'alluvionnement du fleuve Niger moyen.* Master's Thesis, Thèse de l'Université de Grenoble.

Angulo-Jaramillo, R., Bagarello, V., & Lassabatere, L. (2016). *Infiltration Measurements for*

Soil Hydraulic Characterization. Springer.

Atta, S., Achard, F., & Mohamedou, S. (2010). Evolution récente de la population, de l'occupation des sols et de la diversité floristique sur un terroir agricole du Sud-Ouest du Niger. *Sciences & Nature, 7,* 119-129. https://doi.org/10.4314/scinat.v7i2.59948

Autovino, D., Rallo, G., & Provenzano, G. (2018). Predicting Soil and Plant Water Status Dynamic in Olive Orchards under Different Irrigation Systems with Hydrus-2D: Model Performance and Scenario Analysis. *Agricultural Water Management, 203,* 225-235. https://doi.org/10.1016/j.agwat.2018.03.015

Bagarello, V., & Iovino, M. (2013). Testing the BEST Procedure to Estimate the Soil Water Retention Curve. *Geoderma, 187,* 67-76. https://doi.org/10.1016/j.geoderma.2012.04.006

Bagarello, V., Di Prima, S., & Iovino, M. (2014). Comparing Alternative Algorithms to Analyze the Beerkan Infiltration Experiment. *Soil Science Society of America Journal, 78,* 724-736. https://doi.org/10.2136/sssaj2013.06.0231

Bagarello, V., Di Prima, S., & Iovino, M. (2017). Estimating Saturated Soil Hydraulic Conductivity by the near Steady-State Phase of a Beerkan Infiltration Test. *Geoderma, 303,* 70-77. https://doi.org/10.1016/j.geoderma.2017.04.030

Bagarello, V., Di Prima, S., Iovino, M., & Provenzano, G. (2012). Estimating Field-Saturated Soil Hydraulic Conductivity by a Simplified Beerkan Infiltration Experiment. *Hydrological Processes, 28,* 1095-1103. https://doi.org/10.1002/hyp.9649

Ballouche, A., & Taïbi, A. N. (2013). Le «dessèchement» de l'Afrique sahélienne: Un leitmotiv du discours d'expert revisité. *Autrepart, 65,* 47-66. https://doi.org/10.3917/autr.065.0047

Barké, M. K., Tychon, B., Ousseini, I., Ozer, A., & Bielders, C. (2017). Détection des cuvettes oasiennes du centre-est du Niger par classification d'images-satellite SPOT5-THX. *European Journal of Applied Remote Sensing, 53,* 32-84.

Barmo, S., Amani, A., Idrissa, A., Bachir, M. M., & Mahamane, A. (2021). Cartographie et dynamique spatio-temporelle des formations végétales de la forêt protégée de Baban Rafi (Niger). *Revue Marocaine des Sciences Agronomiques et Vétérinaires, 9,* 64-72.

Basile, A., Albrizio, R., Autovino, D., Bonfante, A., De Mascellis, R., Terribile, F. et al. (2020). A Modelling Approach to Discriminate Contributions of Soil Hydrological Properties and Slope Gradient to Water Stress in Mediterranean Vineyards. *Agricultural Water Management, 241,* Article ID: 106338. https://doi.org/10.1016/j.agwat.2020.106338

Bassole, Z., Yanogo, I. P., & Idani, F. T. (2023). Caractérisation des sols ferrugineux tropicaux lessivés et des sols bruns eutrophes tropicaux pour l'utilisation agricole dans le bas-fond de Goundi-Djoro (Burkina Faso). *International Journal of Biological and Chemical Sciences, 17,* 247-266. https://doi.org/10.4314/ijbcs.v17i1.18

Bationo, B. A., Dan-Badjo, A. T., & Nomaou, D. L. (2015). Variations Texturales Et Chimiques Autour Des Touffes D'hyphaene Thebaica (Mart) Des Sols Dans La Region De Maradi, Niger [Textural and Chemical Variations around Hyphaene Thebaica (Mart) Tufts of Soils in Maradi Region, Niger]. *Algerian Journal of Arid Environment, 5,* 40-55. https://doi.org/10.12816/0045906

Ben-Hur, M., Yolcu, G., Uysal, H., Lado, M., & Paz, A. (2009). Soil Structure Changes: Aggregate Size and Soil Texture Effects on Hydraulic Conductivity under Different Saline and Sodic Conditions. *Soil Research, 47,* 688-696. https://doi.org/10.1071/sr09009

Bilodeau, E. (2023). *Évaluation de l'impact des changements climatiques sur le ruissellement des bassins versants urbains* (66 p). Master's Thesis. Université du Québec.

Bouzou, I., Moussa, M., Aghali, I., Abdoulaye, B., Mahamadou, B., Oumarou, F., Ibrahim, M., Bachir, A., Descroix, L., Eric, L., & Vandervaere, J. (2020). Dynamique Hydro-Erosive Actuelle Des Bassins Versants Endoreiques De La Region De Niamey (Sud-Ouest Du Niger). *European Scientific Journal, ESJ, 16,* 149. https://doi.org/10.19044/esj.2020.v16n33p149

Brüning, L., & Piguet, E. (2018). Changements environnementaux et migration en Afrique de l'Ouest. Une revue des études de cas. *Belgeo, 1,* 26. https://doi.org/10.4000/belgeo.28836

Bullard, J. E., Ockelford, A., Strong, C. L., & Aubault, H. (2018). Impact of Multi-Day Rainfall Events on Surface Roughness and Physical Crusting of Very Fine Soils. *Geoderma, 313,* 181-192. https://doi.org/10.1016/j.geoderma.2017.10.038

Carmi, G., & Berliner, P. (2008). The Effect of Soil Crust on the Generation of Runoff on Small Plots in an Arid Environment. *CATENA, 74,* 37-42. https://doi.org/10.1016/j.catena.2008.02.002

Carrick, S., Buchan, G., Almond, P., & Smith, N. (2011). Atypical Early-Time Infiltration into a Structured Soil near Field Capacity: The Dynamic Interplay between Sorptivity, Hydrophobicity, and Air Encapsulation. *Geoderma, 160,* 579-589. https://doi.org/10.1016/j.geoderma.2010.11.006

Casenave, A., & Valentin, C. (1989). *Les états de surface de la zone sahélienne; influence sur l'infiltration* (p. 229). ORS TOM.

Chahinian, N., Voltz, M., Moussa, R., & Trotoux, G. (2006). Assessing the Impact of the Hydraulic Properties of a Crusted Soil on Overland Flow Modelling at the Field Scale. *Hydrological Processes, 20,* 1701-1722. https://doi.org/10.1002/hyp.5948

Coq, S., Barthès, B. G., Oliver, R., Rabary, B., & Blanchart, E. (2007). Earthworm Activity Affects Soil Aggregation and Organic Matter Dynamics According to the Quality and Localization of Crop Residues—An Experimental Study (Madagascar). *Soil Biology and Biochemistry, 39,* 2119-2128. https://doi.org/10.1016/j.soilbio.2007.03.019

Darboux, F., Legout, A., Pousse, N., & Algayer, B. (2024). L'érosion: Des mécanismes à une méthode générale de réduction. *Rendez-vous Techniques de l'ONF, 79,* 5-13.

Descroix, L., & Nouvelot, J. (1997). Aridité et sécheresses du Nord-Mexique (pt. 1). *Revista Trace, No. 30,* 9-16. https://doi.org/10.22134/trace.30.1996.700

Descroix, L., Diongue Niang, A., Panthou, G., Bodian, A., Sane, Y., Dacosta, H. et al. (2015). Évolution récente de la pluviométrie en Afrique de l'ouest à travers deux régions: La Sénégambie et le bassin du Niger moyen. *Climatologie, 12,* 25-43. https://doi.org/10.4267/climatologie.1105

Descroix, L., Guichard, F., Grippa, M., Lambert, L. A., Panthou, G., Mahé, G. et al. (2018). Evolution of Surface Hydrology in the Sahelo-Sudanian Strip: An Updated Review. *Water, 10,* Article 748. https://doi.org/10.3390/w10060748

Descroix, L., Mamadou, I., Abdou, M. M., Bachir, A., Moussa, I. B., Le Breton, E. et al. (2012). État des lieux et proposition de restauration des sols sur le Bassin versant de Tondi Kiboro (Niger). In E. Roose, H. Duchaufour, & G. De Noni (Eds.), *Lutte antiérosive: Réhabilitation des sols tropicaux et protection contre les pluies exceptionnelles* (10 p). IRD Éditions. https://doi.org/10.4000/books.irdeditions.12983

Di Prima, S. (2015). Automated Single Ring Infiltrometer with a Low-Cost Microcontroller Circuit. *Computers and Electronics in Agriculture, 118,* 390-395. https://doi.org/10.1016/j.compag.2015.09.022

Di Prima, S., Lassabatere, L., Bagarello, V., Iovino, M., & Angulo-Jaramillo, R. (2016). Testing a New Automated Single Ring Infiltrometer for Beerkan Infiltration Experiments.

Geoderma, 262, 20-34. https://doi.org/10.1016/j.geoderma.2015.08.006

Edahbi, M., Khaddor, M., & Salmoun, F. (2014). Caractérisation des sols du Nord du Maroc (Bassin Loukkos). *Journal of Environmental Sciences, 5,* 2133-2138.

El Bakkari, M. (2025). Évolution de la sante vegetale et impacts de l'erosion dans la region d'Oueltana Amont (Maroc): Une analyse basee sur l'indice NDVI. *Revista de Estudios Andaluces, 49,* 112-119. https://doi.org/10.12795/rea.2025.i49.06

El Mazi, M., Hmamouchi, M., & Houari, A. (2021). Impact de l'évolution de l'utilisation des terres sur la dégradation des ressources en sols dans le Rif Central méridional, Maroc. *Revue Marocaine des Sciences Agronomiques et Vétérinaires, 9,* 567-572.

Fan, Y., Lei, T., Shainberg, I., & Cai, Q. (2008). Wetting Rate and Rain Depth Effects on Crust Strength and Micromorphology. *Soil Science Society of America Journal, 72,* 1604-1610. https://doi.org/10.2136/sssaj2007.0334

Farzamian, M., Autovino, D., Basile, A., De Mascellis, R., Dragonetti, G., Monteiro Santos, F. et al. (2021). Assessing the Dynamics of Soil Salinity with Time-Lapse Inversion of Electromagnetic Data Guided by Hydrological Modelling. *Hydrology and Earth System Sciences, 25,* 1509-1527. https://doi.org/10.5194/hess-25-1509-2021

Favreau, G. (2000). *Caractérisation et modélisation d'une nappe phréatique en hausse au Sahel.* Master's Thesis, Université Paris XI.

Fernández-Gálvez, J., Pollacco, J. A. P., Lassabatere, L., Angulo-Jaramillo, R., & Carrick, S. (2019). A General Beerkan Estimation of Soil Transfer Parameters Method Predicting Hydraulic Parameters of Any Unimodal Water Retention and Hydraulic Conductivity Curves: Application to the Kosugi Soil Hydraulic Model without Using Particle Size Distribution Data. *Advances in Water Resources, 129,* 118-130. https://doi.org/10.1016/j.advwatres.2019.05.005

Fiorillo, E., Maselli, F., Tarchiani, V., & Vignaroli, P. (2017). Analysis of Land Degradation Processes on a Tiger Bush Plateau in South West Niger Using MODIS and LANDSAT TM/ETM+ Data. *International Journal of Applied Earth Observation and Geoinformation, 62,* 56-68. https://doi.org/10.1016/j.jag.2017.05.010

Folega, F., Atakpama, W., Wala, K., Mukete, B., Shozo, S., Akira, O. et al. (2019). Land Use Patterns and Tree Species Diversity in the Volta Geological Unit, Togo. *Journal of Mountain Science, 16,* 1869-1882. https://doi.org/10.1007/s11629-018-5154-4

Fusco, M., Alagna, V., Autovino, D., Caltabellotta, G., Iovino, M., Vaccaro, G. et al. (2024). Comparing Mini-Disk Infiltrometer, BEST Method and Soil Core Estimates of Hydraulic Conductivity of a Sandy-Loam Soil. *Soil and Tillage Research, 244,* Article ID: 106263. https://doi.org/10.1016/j.still.2024.106263

Gal, L., Grippa, M., Hiernaux, P., Pons, L., & Kergoat, L. (2017). The Paradoxical Evolution of Runoff in the Pastoral Sahel: Analysis of the Hydrological Changes over the Agoufou Watershed (Mali) Using the KINEROS-2 Model. *Hydrology and Earth System Sciences, 21,* 4591-4613. https://doi.org/10.5194/hess-21-4591-2017

Garenne, M., & Ferdi, S. F. (2016). *La pression de la population dans les Pays Sahéliens Francophones: Analyse des estimations et projections de population* (26 p). Ferdi Working Paper, No. 168.

Gavaud, M. (1968). *Les sols bien drainés sur matériaux sableux du Niger essai de systématique régionale* (pp. 278-307). ORSTOM VI.

Gavaud, M. (1977). *Les grands traits de la pédogenèse au Niger méridional. Travaux et documents de l'Orstom, 76.* Orstom Éditions.

Giannini, A., Salack, S., Lodoun, T., Ali, A., Gaye, A. T., & Ndiaye, O. (2013). A Unifying View of Climate Change in the Sahel Linking Intra-Seasonal, Interannual and Longer

Time Scales. *Environmental Research Letters, 8,* Article ID: 024010. https://doi.org/10.1088/1748-9326/8/2/024010

Guengant, J. P., & Banoin, M. (2003). *Dynamique des populations, disponibilité en terres et adaptation des régimes fonciers: Le cas du Niger* (p. 144). FAO, CICRED.

Habou, Z. A., Boubacar, M. K., & Adam, T. (2016). Les systèmes de productions agricoles du Niger face au changement climatique: Défis et perspectives. *International Journal of Biological and Chemical Sciences, 10,* 1262-1272. https://doi.org/10.4314/ijbcs.v10i3.28

Hado, H. A., Adamou, M. M., Hima, K., Favreau, G., Boucher, M., & Dano, I. D. (2021). Rise of Urban Water Table as a Cause of Flooding: Improving Knowledge in the City of Niamey (Niger Republic). *Journal of Water Resource and Protection, 13,* 976-999. https://doi.org/10.4236/jwarp.2021.1312053

Håkansson, I., & Medvedev, V. W. (1995). Protection of Soils from Mechanical Overloading by Establishing Limits for Stresses Caused by Heavy Vehicles. *Soil and Tillage Research, 35,* 85-97. https://doi.org/10.1016/0167-1987(95)00476-9

Halidou, D. H., Abdou, M. M., & Mayaki, Z. A. (2020). Caractérisation du sol du site dégradé de Sakey koira Tegui au Niger pour un meilleur reboisement avec*Acacia senegal*. *International Journal of Biological and Chemical Sciences, 14,* 1470-1478. https://doi.org/10.4314/ijbcs.v14i4.24

Hamadou Younoussa, B., Yaou, T. H., Touré, A. A., Mamoudou Jaoudar, Z., & Garba, Z. (2018). Dégradation des terres et évaluation du potentiel physicochimique des terres dégradées du Sudouest du Niger: Cas des sols du terroir villageois de Boubon. *Revue Ivoirienne des Sciences et Technologie, 31,* 123-137.

Hiernaux, P., & Le Houérou, H. N. (2006). Dynamique de la végétation sahélienne. Bilan du suivi des sites pastoraux du Gourma en 1992. *Science et changements planétaires/Sécheresse, 17,* 51-71.

Hiernaux, P., Ayantunde, A., Kalilou, A., Mougin, E., Gérard, B., Baup, F. et al. (2009). Trends in Productivity of Crops, Fallow and Rangelands in Southwest Niger: Impact of Land Use, Management and Variable Rainfall. *Journal of Hydrology, 375,* 65-77. https://doi.org/10.1016/j.jhydrol.2009.01.032

Horton, R. (1933). *Trans. Am. Geophys. Union 14 446-60 IPCC 2013 Climate Change 2013: The Physical Science Basis Contribution of Working Group I to the Fifth Assessment Report of the Intergovernmental Panel on Climate Change Ed T F Stocker, D Qin, G K Plattner, M Tignor, S K Allen, J Boschung, A Nauels, Y Xia, V Bex and P M Midgley.* Cambridge University Press.

Idé, I. (2022). *Dynamique des flux éoliens sur le complexe dunaire de Namaro (Sud-Ouest du Niger): Impacts des usages de sol, des variations de la végétation et du climat.* Master's Thesis, Université Abdou Moumouni Niamey.

INS-Niger (2018). *Le tableau de bord social* (p. 97).

Issa, A., Nourou, M., Kiari, S. A., Aissata, M. I., Oumani, A. A., & Jens, A. B. (2020). Effets combinés des doses croissantes de fientes de poules associées à la cendre, des placement et sarclage mécaniques et de traitements de semences sur la performance du mil au Niger. *Afrique Science, 17,* 67-82.

Jiang, C., Zhao, L., Dai, J., Liu, H., Li, Z., Wang, X. et al. (2020). Examining the Soil Erosion Responses to Ecological Restoration Programs and Landscape Drivers: A Spatial Econometric Perspective. *Journal of Arid Environments, 183,* Article ID: 104255. https://doi.org/10.1016/j.jaridenv.2020.104255

Kabore, P. N., Ouedraogo, A., Sanon, M., Yaka, P., & Some, L. (2017). Caractérisation de la variabilité climatique dans la region du centre-nord du burkina faso entre 1961 et 2015.

Climatologie, 14, 82-95. https://doi.org/10.4267/climatologie.1268

Kaiser, D., Lepage, M., Konaté, S., & Linsenmair, K. E. (2017). Ecosystem Services of Termites (Blattoidea: Termitoidae) in the Traditional Soil Restoration and Cropping System Zaï in Northern Burkina Faso (West Africa). *Agriculture, Ecosystems & Environment, 236,* 198-211. https://doi.org/10.1016/j.agee.2016.11.023

Khelifa, W. B., Hermassi, T., Strohmeier, S., Zucca, C., Ziadat, F., Boufaroua, M. et al. (2017). Parameterization of the Effect of Bench Terraces on Runoff and Sediment Yield by Swat Modeling in a Small Semi-Arid Watershed in Northern Tunisia. *Land Degradation & Development, 28,* 1568-1578. https://doi.org/10.1002/ldr.2685

Kinnell, P. I. A. (2012). Raindrop-Induced Saltation and the Enrichment of Sediment Discharged from Sheet and Interrill Erosion Areas. *Hydrological Processes, 26,* 1449-1456. https://doi.org/10.1002/hyp.8270

Knödel, K., Lange, G., & Voigt, H. J. (2007). *Environmental Geology.* Springer.

L'Hôte, Y., Mahé, G., Somé, B., & Triboulet, J. P. (2002). Analysis of a Sahelian Annual Rainfall Index from 1896 to 2000; the Drought Continues. *Hydrological Sciences Journal, 47,* 563-572. https://doi.org/10.1080/02626660209492960

Lavelle, P., Pashanasi, B., Charpentier, F., Gilot, C., Rossi, J. P., Derouard, L., André, J., Ponge, J. F., & Bernier, N. (1998). *Large-Scale Effects of Earthworms on Soil Organic Matter and Nutrient Dynamics.* St. Lucie Press.

Lebel, T., & Ali, A. (2009). Recent Trends in the Central and Western Sahel Rainfall Regime (1990-2007). *Journal of Hydrology, 375,* 52-64. https://doi.org/10.1016/j.jhydrol.2008.11.030

Leblanc, M. J., Favreau, G., Massuel, S., Tweed, S. O., Loireau, M., & Cappelaere, B. (2007). Land Clearance and Hydrological Change in the Sahel: SW Niger. *Global and Planetary Change, 61,* 135-150. https://doi.org/10.1016/j.gloplacha.2007.08.011

Leduc, C., Favreau, G., & Schroeter, P. (2001). Long-Term Rise in a Sahelian Water-Table: The Continental Terminal in South-West Niger. *Journal of Hydrology, 243,* 43-54. https://doi.org/10.1016/s0022-1694(00)00403-0

Leonard, J., & Rajot, J. L. (2000). Influence of Termites on Runoff and Infiltration: Quantification and Analysis. *Geoderma, 104,* 17-40. https://doi.org/10.1016/s0016-7061(01)00054-4

Li, Z., & Fang, H. (2016). Impacts of Climate Change on Water Erosion: A Review. *Earth-Science Reviews, 163,* 94-117. https://doi.org/10.1016/j.earscirev.2016.10.004

Lin, L., Lonla, P. Y., Vijayakumar, J., Khan, M. K., Di Emidio, G., Krekelbergh, N. et al. (2025). Soil Surface Properties and Infiltration Response to Crust Forming of a Sandy Loam and Silt Loam. *Soil and Tillage Research, 248,* Article ID: 106440. https://doi.org/10.1016/j.still.2024.106440

Liu, Y., Liu, Y., Wu, G., & Shi, Z. (2019). Runoff Maintenance and Sediment Reduction of Different Grasslands Based on Simulated Rainfall Experiments. *Journal of Hydrology, 572,* 329-335. https://doi.org/10.1016/j.jhydrol.2019.03.008

Lubès-Niel, H., Séguis, L., & Sabatier, R. (2001). Étude de stationnarité des caractéristiques des événements pluvieux de la station de Niamey sur la période 1956-1998. *Comptes Rendus de l'Académie des Sciences—Series IIA—Earth and Planetary Science, 333,* 645-650. https://doi.org/10.1016/s1251-8050(01)01690-1

Mahamadou Moudi, R., Djamilou, O. A., Amadou, A. B., & Kabirou, S. (2024). Contraintes et stratégies de protection de Hyphaene thebaica (Palmier Doum) dans la Commune Rurale de Gazaoua au Niger. *Revue Ecosystèmes et Paysages, 4,* 1-10.

https://doi.org/10.59384/recopays.tg4221

Mahamadou, A., Ismaël, A. B., Garba, I., & Nafissatour, H. M. (2023). Analysis of Land Use Dynamics and Economic Impacts of Sustainable Land Management in the Tillaberi Region of Niger. *International Journal of Innovation and Applied Studies, 39,* 595-60. http://www.ijias.issr-journals.org/

Maigari, M. A., Ambouta, K. J. M., Bielders, C. L., & Tidjani, A. D. (2018). Caractérisation de la végétation des dunes dégradées du Sud-est du Niger. *Environmental and Water Sciences, 2,* 83-94.

Malam Abdou, M. (2014). *Etats de surface et fonctionnement hydrodynamique multi-échelles des bassins Sahéliens; études expérimentales en zones cristalline et sédimentaire. Sciences de la terre* (268 p). Ph.D. Thesis, Université de Grenoble.

Malam Abdou, M. (2016). Hausse des écoulements sur le bassin versant de Dargol: Entre facteurs anthropiques et climatiques. *Revue de Géographie de l'Université Ouaga I Pr Joseph KI-ZERBO, 2,* 19-44.

Malam Issa, O., Défarge, C., Trichet, J., Valentin, C., & Rajot, J. L. (2009). Microbiotic Soil Crusts in the Sahel of Western Niger and Their Influence on Soil Porosity and Water Dynamics. *CATENA, 77,* 48-55. https://doi.org/10.1016/j.catena.2008.12.013

Malam Issa, O., Trichet, J., Défarge, C., Couté, A., & Valentin, C. (1999). Morphology and Microstructure of Microbiotic Soil Crusts on a Tiger Bush Sequence (Niger, Sahel). *CATENA, 37,* 175-196. https://doi.org/10.1016/s0341-8162(99)00052-1

Malam Issa, O., Valentin, C., Rajot, J. L., Cerdan, O., Desprats, J., & Bouchet, T. (2011). Runoff Generation Fostered by Physical and Biological Crusts in Semi-Arid Sandy Soils. *Geoderma, 167,* 22-29. https://doi.org/10.1016/j.geoderma.2011.09.013

Mamadou, I. (2012). *La dynamique accélérée des koris de la région de Niamey et ses conséquences sur l'ensablement du fleuve Niger.* Master's Thesis, Université Abdou Moumouni.

Mamadou, I., Gautier, E., Descroix, L., Noma, I., Bouzou Moussa, I., Faran Maiga, O. et al. (2015). Exorheism Growth as an Explanation of Increasing Flooding in the Sahel. *CATENA, 131,* 130-139. https://doi.org/10.1016/j.catena.2015.03.017

Maman Aminou, A. A. (2023). *Impact des changements climatiques et environnementaux sur les ressources naturelles dans les bassins versants du complexe limnique Kongou-Saga gorou: Sud-ouest du Niger.* Master's Thesis, Université Abdou Moumouni Niamey.

Maman Aminou, A. A., Garba, Z., & Touré, A. A. (2019). Dynamique de la conductivité dans les eaux de surface et souterraines du Sud-ouest du Niger: cas du lac et puits de Yaboni. *Revue Ivoirienne des Sciences et Technologie, 34,* 389-404. http://www.revist.ci

Martínez-Mena, M., Carrillo-López, E., Boix-Fayos, C., Almagro, M., García Franco, N., Díaz-Pereira, E. et al. (2020). Long-Term Effectiveness of Sustainable Land Management Practices to Control Runoff, Soil Erosion, and Nutrient Loss and the Role of Rainfall Intensity in Mediterranean Rainfed Agroecosystems. *CATENA, 187,* Article ID: 104352. https://doi.org/10.1016/j.catena.2019.104352

Mathilde, D. F. (2023). *Suivi des plans d'eau en Afrique de l'Ouest par télédétection: Analyse du régime hydrologique par une approche multi-capteurs et classification par réseau de neurones.* Master's Thesis, Université Paul Sabatier—Toulouse III Français.

Medinski, T. V., Mills, A. J., & Fey, M. V. (2009). Relationships between Soil Particle Size Fractions and Infiltrability. *South African Journal of Plant and Soil, 26,* 147-156. https://doi.org/10.1080/02571862.2009.10639948

Messager, M. L., Lehner, B., Grill, G., Nedeva, I., & Schmitt, O. (2016). Estimating the Volume and Age of Water Stored in Global Lakes Using a Geo-Statistical Approach. *Nature*

Communications, 7, Article No. 13603. https://doi.org/10.1038/ncomms13603

Millogo, D., Nikiema, A., Koulibaly, B., & Zombre, N. P. (2017). Analyse de l'évolution de l'occupation des terres à partir de photographies aériennes de la localité de Loaga dans la province du Bam, Burkina Faso. *International Journal of Biological and Chemical Sciences, 11,* 2133-2143. https://doi.org/10.4314/ijbcs.v11i5.16

Morsli, B., Mazour, M., Mededjel, N., Hamoudi, A., & Roosé, E. (2004). Influence de l'utilisation des terres sur les risques de ruissellement et d'érosion sur les versants semi-arides du nord-ouest de l'Algérie. *Sécheresse, 15,* 96-104.

Mounirou, L. A. (2012). *Etude du ruissellement et de l'érosion à différentes échelles spatiales sur le bassin versant de Tougou en zone sahélienne du Burkina Faso: quantification et transposition des données.* Master's Thesis, Montpellier 2 University.

Moussa Boubacar, M. (2023). *Qualité des eaux de surface de la zone de Niamey: Caractérisation physico-chimiques, dynamique spatio-temporelle des concentrations (MES) et en bactéries d'origines fécale (E. coli).* Master's Thesis, Université Paul Sabatier-Toulouse III.

Moussa Issaka, A. (2014). *Dynamiques érosives et des états de surfaces dans la partie nigérienne du bassin lac Tchad.* Master's Thesis, Université Abdou Moumouni de Niamey.

Mrabet, S. A. B., Hachichi, A., Taibi, S., & Fleureau, J. (2010). Conductivité hydraulique non saturée de l'argile de Mers El Kébir (Algérie). *European Journal of Environmental and Civil Engineering, 14,* 1297-1315. https://doi.org/10.1080/19648189.2010.9693295

Mvondo-Awono, J., Lawane, P., Boukong, A., Mvondozé, A. D., & Beyegue-Djonko, H. (2013). Rétablissement de la capacité de production de sorgho (*Sorghum bicolor* [L.] Moench) d'un vertisol dégradé dans la région de l'Extrême Nord du Cameroun. *Biotechnology, Agronomy, Society and Environment, 17,* 56-63.

Neave, M., & Rayburg, S. (2007). A Field Investigation into the Effects of Progressive Rainfall-Induced Soil Seal and Crust Development on Runoff and Erosion Rates: The Impact of Surface Cover. *Geomorphology, 87,* 378-390. https://doi.org/10.1016/j.geomorph.2006.10.007

Ngo, P. T., Rumpel, C., Dignac, M., Billou, D., Duc, T. T., & Jouquet, P. (2011). Transformation of Buffalo Manure by Composting or Vermicomposting to Rehabilitate Degraded Tropical Soils. *Ecological Engineering, 37,* 269-276. https://doi.org/10.1016/j.ecoleng.2010.11.011

Niang D., Mermoud, A., Yacouba, H., & Karambiri, H. (2004). Fonctionnement hydrique de différents types de formations éoliennes en milieu sahélien burkinabé. *SUD Sciences & Technologies, No. 12,* 4-12.

Nicholson, S. E. (2011). *Dryland Climatologie* (p. 516). Cambridge University Press.

Noma Adamou, S. (2022). *Érosion hydrique dans le bassin versant du kori Ouallam (Sud-Ouest du Niger): Caractérisations physico-chimique et Minéralogique des couvertures pédologiques, modélisation et impacts des aménagements antiérosifs sur les écosystèmes.* Master's Thesis, Université Cadi Ayyad, de Marrakech.

Noma Adamou, S., Daoudi, L., & Abdourhamane Touré, A. (2024b). Dynamique d'occupation des sols et perception paysanne au Sud-ouest du Niger: Cas du bassin versant du Kori Ouallam. *European Scientific Journal, ESJ, 20,* 163-189. https://doi.org/10.19044/esj.2024.v20n35p163

Noma Adamou, S., Daoudi, L., Abdourhamane Touré, A., & Fagel, N. (2024a). Origin and Distribution of Clay Minerals in Semi-Arid Sahelian Soils: Case of Kori Ouallam Watershed, South-Western Niger. *Clay Minerals, 59,* 213-227. https://doi.org/10.1180/clm.2024.21

Noma Adamou, S., Gourfi, A., Touré, A. A., & Daoudi, L. (2022). Érosion hydrique au sud-ouest du Niger: Impacts des facteurs naturels et anthropiques sur les pertes en sols. *Géomorphologie: Relief, processus, environnement, 28,* 77-92. https://doi.org/10.4000/geomorphologie.16744

Oumani, A. H. (2023). Femmes et gouvernance. In M. C. Chalus-Sauvannet (Ed.), *Femmes et gouvernance* (pp. 181-201). EMS Editions. https://doi.org/10.3917/ems.chalu.2023.01.0181

Ozer, P., & Perrin, D. (2014). Eau et changement climatique. Tendances et perceptions en Afrique de l'Ouest. In A. Ballouche, & N. A. Taibi (Eds.), *Eau, milieux et aménagement. Une recherche au service des territoires* (pp. 227-245). Presses de l'Université d'Angers.

Panthou, G., Lebel, T., Vischel, T., Quantin, G., Sane, Y., Ba, A. et al. (2018). Rainfall Intensification in Tropical Semi-Arid Regions: The Sahelian Case. *Environmental Research Letters, 13,* Article ID: 064013. https://doi.org/10.1088/1748-9326/aac334

Panthou, G., Vischel, T., & Lebel, T. (2014). Recent Trends in the Regime of Extreme Rainfall in the Central Sahel. *International Journal of Climatology, 34,* 3998-4006. https://doi.org/10.1002/joc.3984

Pi, X., Luo, Q., Feng, L., Xu, Y., Tang, J., Liang, X. et al. (2022). Mapping Global Lake Dynamics Reveals the Emerging Roles of Small Lakes. *Nature Communications, 13,* Article No. 5777. https://doi.org/10.1038/s41467-022-33239-3

Potts, M., & Graves, A. (2013). Big Issues Deserve Blod Responses. Population and Climate Change in the Sahel. *Africans Journals of Reproductive Health, 17,* 9-14.

Rabouli, S. (2022). *Méthode innovante de spatialisation des propriétés physiques du sol: Application aux surfaces d'infiltration. Ingénierie de l'environnement.* Master's Thesis, Université de Lyon Français.

Radcliffe, D. E., & Simunek, J. (2010). *Soil Phisics with HYDRUS, Modelling and Applications* (p. 373). CRC Press Taylor & Francis Group.

Rajot, J., Karambiri, H., Ribolzi, O., Planchon, O., & Thiebaux, J. (2009). Interaction entre érosions hydrique et éolienne sur sols sableux pâturés au Sahel: Cas du bassin-versant de Katchari au nord du Burkina Faso. *Sécheresse, 20,* 131-138. https://doi.org/10.1684/sec.2009.0171

Ran, Q., Shi, Z., Fu, X., Wang, G., & Xu, Y. (2012). Impact of Rainfall Movement on Soil Crust Development. *International Journal of Sediment Research, 27,* 439-450. https://doi.org/10.1016/s1001-6279(13)60003-7

Reynolds, W. D., & Elrick, D. E. (1990). Ponded Infiltration from a Single Ring: I. Analysis of Steady Flow. *Soil Science Society of America Journal, 54,* 1233-1241. https://doi.org/10.2136/sssaj1990.03615995005400050006x

Reynolds, W. D., & Elrick, D. E. (2002). Hydraulic Conductivity of Saturated Soils, Constant Head Method. In *Methods of Soil Analyses, Part 4, Physical Methods, Book Series 5* (pp. 694-700). Soil Science Society of America.

Rienzi, E. A., Fox, J. F., Grove, J. H., & Matocha, C. J. (2013). Interrill Erosion in Soils with Different Land Uses: The Kinetic Energy Wetting Effect on Temporal Particle Size Distribution. *CATENA, 107,* 130-138. https://doi.org/10.1016/j.catena.2013.02.007

Robert, E. (2011). *Les risques de pertes en terre et en eau dans le bassin versant de la Doubégué (Burkina Faso): Pour une gestion intégrée.* Master's Thesis, Université Michel de Montaigne—Bordeaux 3.

Robert, W., Reij, C., Garrity, D., Glover, J., Hellums, D., Megahuey, M., & Scherr, S. (2017). Amélioration de la gestion des terres et des eaux. In *World Ressources Institute «création d'un avenir alimentaire durable» épisode 4* (p. 44).

Roose, E. (1999). *Introduction à la gestion conservatoire de l'eau, de la biomasse et de la fertilité des sols (GCES)* (p. 420). Bulletin Pédologique de la FAO N°70, FAO/IRD.

Sadda, A. S., Diouf, A., Lawali, S., Ouedraogo, M., Bogaert, J., & Mahamane, A. (2016). Pression anthropique et dynamique paysagére en zone rurale semi-aride: Cas de la commune de Tibiri, région de Maradi (Niger). *Tropicultura, 34,* 127-139.

Sanogo, S., Fink, A. H., Omotosho, J. A., Ba, A., Redl, R., & Ermert, V. (2015). Spatio-temporal Characteristics of the Recent Rainfall Recovery in West Africa. *International Journal of Climatology, 35,* 4589-4605. https://doi.org/10.1002/joc.4309

Seck, M. B., & Sy, B. A. (2021). Potentiels agronomiques des Niayes de Mboro (littoral Nord du Sénégal) et risques de dégradation mécanique par ensablement: Approche par analyse géomorphologique des enjeux socio-économiques. *European Scientific Journal ESJ, 17,* 140. https://doi.org/10.19044/esj.2021.v17n20p140

Sighomnou, D., Descroix, L., Genthon, P., Mahé, G., Bouzou Moussa, I., Gautier, E. et al. (2013). The Niger River Niamey Flood of 2012: The Paroxysm of the Sahelian Paradox? *Sécheresse, 24,* 3-13. https://doi.org/10.1684/sec.2013.0370

Taylor, C. M., Belušić, D., Guichard, F., Parker, D. J., Vischel, T., Bock, O. et al. (2017). Frequency of Extreme Sahelian Storms Tripled since 1982 in Satellite Observations. *Nature, 544,* 475-478. https://doi.org/10.1038/nature22069

Tidiane Dia, A., Ndiaye, P. M., Sougou, A., & Aldiouma Sy, B. (2023). Analyse des déterminants physiques et suivi de la dynamique des écoulements pluviaux liés au ravinement en milieu sahélien: Bassin versant de Ogo (Nord-est du Sénégal). *Revue Espace Géographique et Société Marocaine Numéro, 71,* 95-111.

Traore, B., Guindo, S. S., Tangara, B., Maiga, M. H., Goita, O., & Diawara, B. (2024). Détermination de la dose et fréquence d'irrigation efficiente du blé tendre dans un système de rotation après le riz sur sol hydromorphe «Danga», en zone Office du Niger, Mali. *Afrique Science, 25,* 137-150. http://www.afriquescience.net

Valentin, C., & Bresson, L. (1992). Morphology, Genesis and Classification of Surface Crusts in Loamy and Sandy Soils. *Geoderma, 55,* 225-245. https://doi.org/10.1016/0016-7061(92)90085-l

Vandervaere, J., Vauclin, M., & Elrick, D. E. (2000). Transient Flow from Tension Infiltrometers I. the Two-parameter Equation. *Soil Science Society of America Journal, 64,* 1263-1272. https://doi.org/10.2136/sssaj2000.6441263x

Vischel, T., Panthou, G., Peyrillé, P., Roehrig, R., Quantin, G., Lebel, T. et al. (2019). Precipitation Extremes in the West African Sahel Recent: Évolution and Physical Mechanisms. In V. Venugopal, J. Sukhatme, et al. (Eds.), *Tropical Extremes* (pp. 95-138). Elsevier. https://doi.org/10.1016/b978-0-12-809248-4.00004-2

Wang, Y., Wu, Y., Hu, L., Hicher, P., & Yin, Z. (2025). A Hydraulic Conductivity Model Incorporating Adsorption and Capillarity for Unsaturated/Frozen Soil. *Engineering Geology, 353,* Article ID: 108093. https://doi.org/10.1016/j.enggeo.2025.108093

Xu, Q., Wu, P., Dai, J., Wang, T., Li, Z., Cai, C. et al. (2018). The Effects of Rainfall Regimes and Terracing on Runoff and Erosion in the Three Gorges Area, China. *Environmental Science and Pollution Research, 25,* 9474-9484. https://doi.org/10.1007/s11356-018-1198-9

Yeom, S. (2017). *Influence of Soil Characteristics on Structural Soil Crust Development* (191 p). Ph.D. Thesis, Drexel University.

Zouré, C., Queloz, P., Koïta, M., Niang, D., Fowé, T., Yonaba, R. et al. (2019). Modelling the Water Balance on Farming Practices at Plot Scale: Case Study of Tougou Watershed in Northern Burkina Faso. *CATENA, 173,* 59-70. https://doi.org/10.1016/j.catena.2018.10.002